Electronic Supplementary Material (ESI) for Catalysis Science & Technology.

Supporting Information for

Competitive Isomerization and Catalyst Decomposition During Ring-Closing Metathesis

Charles Killeen, Jie Liu, Harmen S. Zijlstra, Florian Maass, James Piers, Reid Adams, Allen Oliver, and J. Scott McIndoe

Table of Contents:

Other supporting information for this manuscript include the following:

X-ray data for **R5**: uvic1601.cif
X-ray data for **R7**: uvic1602.cif

Experimental

General Procedures

All glassware used for this work was cleaned by immersion in an acid bath, a base bath, and then thoroughly rinsed with deionized water and dried overnight in an oven. All plastic syringes and needles were obtained commercially and single used. All substrate synthesis reactions were carried out in a fume hood under air. All solutions of catalyst and reagents were prepared with dried, degassed solvents either in a glovebox or using Schlenk techniques. Grubbs' second generation catalyst (Sigma-Aldrich, M204), allyl bromide (Sigma-Aldrich, 97 %), 4-bromobut-1-ene (Oakwood Chemical, 98 %), 5-bromopent-1-ene (Oakwood Chemical, 98 %), 6-bromohex-1-ene (Oakwood Chemical, 97 %), 7-bromohept-1-ene (Oakwood Chemical, 98 %), 8-bromooct-1-ene (Oakwood Chemical, 96 %), 11-bromoundec-1-ene (Sigma-Aldrich, 95 %), and dibutylamine (Sigma-Aldrich, 99.5 %) were used without further purification. Dichloromethane (Supelco, HPLC grade, stabilizer-free) was dried over calcium hydride and distilled and degassed before use.

NMR spectra were recorded on a Bruker Avance III 300 Hz NMR spectrometer at standard conditions and referenced to the residual proton or ^{13}C atom of the solvent. NMR chemical shifts are reported in ppm relative to TMS at 0 ppm. Chloroform-d (Sigma-Aldrich, 99.8 atom % D) or dimethyl sulfoxide-d$_6$ (Sigma-Aldrich, 99.9% atom % D) were stored over molecular sieves and used for all ^{1}H and ^{13}C NMR spectra.

All kinetic mass spectrometry experiments were conducted with a Waters Acquity tandem quadrupole detector in positive mode with a capillary voltage of 3.00 kV, a cone voltage of 12 V, and an extraction voltage of 3 V. Optimal desolvation was obtained using a desolvation gas flow of 100 L h^{-1}, cone gas flow of 100 L h^{-1}, source temperature of 50 °C, desolvation gas temperature of 150 °C, and a detector gain of 470 V. Scan time was set to one second, with an inter-scan time of 0.1 seconds.

Experimental Procedure for Kinetics Experiments

Substrate solutions were prepared in a PSI flask[1] in 9 mL dichloromethane in a glovebox or using Schlenk techniques to a total bis-alkene concentration of 3.9 µM. The PSI flask was sealed with a septum and Young's tap and removed from the glovebox/Schlenk line and heated to 40 °C with stirring. Then, under an overpressure of 5 psi of argon (Praxair Canada, 99.999%), the headspace of the PSI flask is briefly purged by puncturing the septum with a needle. A 60 cm length of PEEK tubing (0.127 mm I.D.) is inserted into the PSI flask through the septum and connected to the source of the Waters Acquity tqd. Upon establishing a stable analyte signal, 1 mL of 35 µM solution of Grubbs' second-generation catalyst is added, bringing the total concentration of both catalyst and bis-alkene(s) to 3.5 µM. The combination of 5 psi overpressure and ~60 cm of 0.127 mm I.D. PEEK tubing gives a solution flow rate of about 25 µL/min through the source of the instrument.

Substrate Synthesis

R5

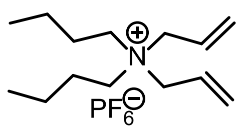

Synthesis of R5: Dibutylamine (337 µL, 2.00 mmol), allyl bromide (381 µL, 4.40 mmol), and potassium carbonate (300 mg, 2.2 mmol) were added to a vial containing 1.5 mL acetonitrile and stirred at room temperature for 23 hours. The resulting cream-coloured slurry was diluted with 15 mL acetonitrile and filtered through a short celite plug. The resulting solution was concentrated *in vacuo* to a volume of 2 mL, and then added to a solution of $NaPF_6$ (420 mg, 2.50 mmol) in 3 mL deionized water, which formed the product as a brown oil. The resulting emulsion was diluted with 15 mL deionized water and extracted with 3×10 mL portions of dichloromethane, which were subsequently dried with Na_2SO_4. The solvent was removed *in vacuo* and the crude residue was purified by crystallization from 10 mL 1:1 water:ethanol. The resulting white powder was collected on a sintered glass filter, washed twice with 5 mL of ice-cold deionized water, and dried, giving the product (391 mg, 1.10 mmol, 55.1% yield). ^{1}H NMR (300 MHz, $CDCl_3$) δ 5.90 (ddt, *J* = 17.2, 14.3, 7.1 Hz, 2H), 5.76 – 5.63 (m, 4H), 3.81 (dd, *J* = 7.0, 1.9 Hz, 4H), 3.19 – 3.07 (m, 4H), 1.77 – 1.60 (m, 4H), 1.48 – 1.29 (m, 4H), 0.97 (t, *J* = 7.3, 1.8 Hz, 6H). ^{13}C{^{1}H} NMR (76 MHz, $CDCl_3$) δ 129.3, 123.6, 61.1, 58.5,23.7, 19.6, 13.6. ESI (+)-MS: *m/z* 210.4.

R6

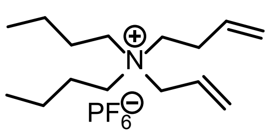

Synthesis of R6: A solution of allyl bromide (5.10 g, 42.2 mmol) in 20 mL diethyl ether was slowly added to dibutylamine (9.81 g, 75.9 mmol) in a 100 mL round-bottom flask at room temperature. The solution was stirred overnight and the resulting white suspension of dibutylammonium bromide was filtered through celite, and then concentrated *in vacuo*. The residue was filtered through celite directly into a 50 mL round-bottom flask and combined with 4-bromo-1-butene (7.10 g, 52.6 mmol), which were then heated to 80 °C with stirring for 72 hours. The resulting brown oil was washed with 3×25 mL portions of diethyl ether, followed by salt metathesis with excess $NaPF_6$ in deionized water. The crude product was isolated as a brown oil and purified by crystallization from ethanol to give a white powder (891 mg, 2.41 mmol, 6.3 % yield (on 0.5 eq. dibutylamine)). ^{1}H NMR (300 MHz, $CDCl_3$) δ 5.97 – 5.62 (m, 4H), 5.30 – 5.13 (m, 2H), 3.86 (d, *J* = 7.0 Hz, 2H), 3.19 (td, *J* = 11.4, 7.7 Hz, 6H), 2.46 (dt, *J* = 12.0, 6.9 Hz, 2H), 1.65 (ddt, *J* = 11.8, 8.7, 5.7 Hz, 4H), 1.40 (h, *J* = 7.3 Hz, 4H), 0.98 (t, *J* = 7.3 Hz, 6H). ^{13}C{^{1}H} NMR (76 MHz, $CDCl_3$) δ 131.1, 129.4, 123.5, 119.7, 61.3, 58.7, 57.6, 26.4, 23.8, 19.6, 13.6. ESI (+)-MS: *m/z* 224.4.

R7

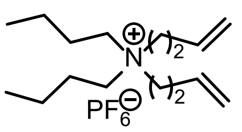

Synthesis of R7: A solution of 4-bromo-1-butene (6.40 g, 44.7 mmol) in 20 mL diethyl ether was slowly added to dibutylamine (9.90 g, 76.7 mmol) in a 100 mL round-bottom flask at room temperature. The solution was stirred overnight and the resulting white suspension of dibutylammonium bromide was filtered through celite, and then concentrated *in vacuo*. The residue was filtered through celite directly into a 50 mL round-bottom flask and combined with 4-bromo-1-butene (7.10 g, 52.6 mmol), which were then heated to 80 °C with stirring for 72 hours. The resulting brown oil was washed with 3×25 mL portions of diethyl ether, followed by salt metathesis with excess $NaPF_6$ in deionized water. The crude product was isolated as a brown oil and purified by crystallization from ethanol to give a white powder (1.15 g, 3.00 mmol, 7.8 % yield (on 0.5 eq. dibutylamine)). ^{1}H NMR (300 MHz, $CDCl_3$) δ 5.72 (ddt, *J* = 16.8, 10.2, 6.6 Hz, 2H), 5.29 – 5.11 (m, 4H), 3.29 – 3.13 (m, 8H), 2.42 (q, *J* = 7.3 Hz, 4H), 1.69 – 1.53

(m, 4H), 1.40 (h, *J* = 7.4 Hz, 4H), 0.97 (t, *J* = 7.3 Hz, 6H). ^{13}C{^{1}H} NMR (76 MHz, CDCl$_3$) δ 131.2, 119.6, 58.9, 57.8, 26.4, 23.8, 19.5, 13.6. ESI (+)-MS: *m/z* 238.5.

R8

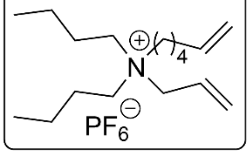

Synthesis of R8: A solution of allyl bromide (5.02 g, 41.8 mmol) in 20 mL diethyl ether was slowly added to dibutylamine (6.82 g, 52.8 mmol) in a 100 mL round-bottom flask at room temperature. The solution was stirred overnight and the resulting white suspension of dibutylammonium bromide was filtered through celite, and then concentrated *in vacuo*. The residue was filtered through celite directly into a 50 mL round-bottom flask and combined with 6-bromo-1-hexene (6.98 g, 42.8 mmol), which were then heated to 80 °C with stirring for 72 hours. The resulting brown oil was washed with 3×25 mL portions of diethyl ether, followed by salt metathesis with excess NaPF$_6$ in deionized water. The crude product was isolated as a brown oil and purified by crystallization from ethanol to give a white powder (1.35 g, 3.40 mmol, 12.9 % yield on 0.5 eq. dibutylamine). ^{1}H NMR (300 MHz, CDCl$_3$) δ 5.95 – 5.62 (m, 4H), 5.12 – 4.95 (m, 2H), 3.82 (d, *J* = 7.0 Hz, 2H), 3.20 – 3.08 (m, 6H), 2.13 (q, *J* = 7.2 Hz, 2H), 1.70 – 1.56 (m, 6H), 1.55 – 1.31 (m, 6H), 0.98 (t, *J* = 7.3 Hz, 6H). ^{13}C{^{1}H} NMR (76 MHz, CDCl$_3$) δ 137.5, 129.2, 123.6, 116.0, 61.1, 58.5, 32.8, 25.2, 23.7, 20.9, 19.6, 13.6. ESI (+)-MS: *m/z* 252.5.

R9

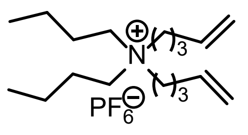

Synthesis of R9: 5-bromo-1-pentene (5.60 g, 37.6 mmol) and dibutylamine (8.14 g, 63.0 mmol) were added to a 100 mL round-bottom flask and stirred neat at 80 °C overnight. The resulting white suspension of dibutylammonium bromide was filtered through celite, and then concentrated *in vacuo*. The residue was filtered through celite directly into a 50 mL round-bottom flask and combined with 5-bromo-1-pentene (6.05 g, 40.6 mmol), which were then heated to 80 °C with stirring for 72 hours. The resulting brown oil was washed with 3×25 mL portions of diethyl ether, followed by salt metathesis with excess NaPF$_6$ in deionized water The crude product was isolated as a brown oil and purified by crystallization from 1-butanol to give a white powder (1.55 g, 3.77 mmol, 12.0 % yield on 0.5 eq. dibutylamine). ^{1}H NMR (300 MHz, CDCl$_3$) δ 5.76 (ddt, *J* = 17.0, 10.2, 6.8 Hz, 2H), 5.20 – 5.04 (m, 4H), 3.21 – 3.09 (m, 8H), 2.16 (qt, *J* = 6.8, 1.3 Hz, 4H), 1.79 – 1.65 (m, 4H), 1.65 – 1.51 (m, 4H), 1.41 (h, *J* = 7.3 Hz, 4H), 0.99 (t, *J* = 7.3 Hz, 6H). ^{13}C{^{1}H} NMR (76 MHz, CDCl$_3$) δ 135.7, 117.7, 58.7, 58.2, 30.0, 23.8, 21.0, 19.6, 13.6. ESI (+)-MS: *m/z* 266.5.

R11

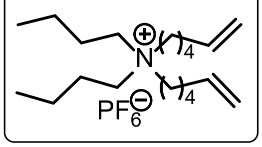

Synthesis of R11: 6-bromo-1-hexene (6.23 g, 38.2 mmol) and dibutylamine (7.03 g, 54.5 mmol) were added to a 100 mL round-bottom flask and stirred neat at 80 °C for 36 h. The resulting white suspension of dibutylammonium bromide was filtered through celite, and then concentrated *in vacuo*. The residue was filtered through celite directly into a 50 mL round-bottom flask and combined with 6-bromo-1-hexene (6.85 g, 42.0 mmol), which were then heated to 80 °C with stirring for 72 hours. The resulting brown oil was washed with 3×25 mL portions of diethyl ether, followed by salt metathesis with excess NaPF$_6$ in deionized water The crude product was isolated as a brown oil and purified by crystallization from 1-butanol to give a white powder (1.71 g, 3.90 mmol, 14.3 % yield (on 0.5 eq. dibutylamine)). ^{1}H NMR (300 MHz, CDCl$_3$) δ 5.75 (ddt, *J* = 16.9, 10.2, 6.7 Hz, 2H), 5.13 – 4.94 (m, 4H), 3.20 – 3.08 (m, 8H), 2.13 (qt, *J* = 6.8, 1.4 Hz, 4H), 1.72 – 1.32 (m, 16H), 0.99 (t, *J* = 7.3 Hz, 6H). ^{13}C{^{1}H} NMR (76 MHz, CDCl$_3$) δ 137.4, 116.1, 58.6, 32.8, 25.2, 23.8, 20.9, 19.7, 13.6. ESI (+)-MS: *m/z* 294.5.

R13

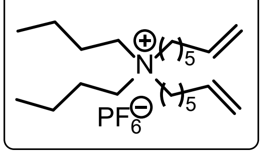

Synthesis of R13: 7-bromo-1-heptene (6.56 g, 37.0 mmol) and dibutylamine (6.01 g, 46.5 mmol) were added to a 100 mL round-bottom flask and stirred neat at 80 °C for 36 h. The resulting white suspension of dibutylammonium bromide was filtered through celite, and then concentrated *in vacuo*. The residue was filtered through celite directly into a 50 mL round-bottom flask and combined with 7-bromo-1-heptene (7.06 g, 39.9 mmol), which were then heated to 80 °C with stirring for 72 hours. The resulting brown oil was washed with 3×25 mL portions of diethyl ether, followed by salt metathesis with excess $NaPF_6$ in deionized water The crude product was isolated as a brown oil and purified by crystallization from 1-butanol to give a white powder (1.53 g, 3.27 mmol, 14.1 % yield (on 0.5 eq. dibutylamine)). ^1H NMR (300 MHz, $CDCl_3$) δ 5.71 (ddt, *J* = 16.8, 9.8, 6.8 Hz, 2H), 5.00 – 4.84 (m, 4H), 3.07 (dt, *J* = 13.3, 4.9 Hz, 8H), 2.00 (q, *J* = 6.5 Hz, 4H), 1.54 (h, *J* = 7.6 Hz, 8H), 1.34 (tq, *J* = 9.6, 5.1 Hz, 12H), 0.92 (t, *J* = 7.3 Hz, 6H).$^{13}C\{^1H\}$ NMR (76 MHz, $CDCl_3$) δ 138.2, 115.1, 58.7, 58.5, 33.4, 28.1, 25.6, 23.8, 21.7, 19.6, 13.6. ESI (+)-MS: *m/z* 322.6.

R15

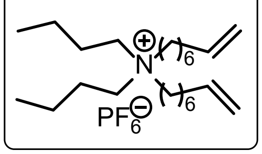

Synthesis of R15: 8-bromo-1-octene (7.18 g, 37.6 mmol) and dibutylamine (6.23 g, 48.2 mmol) were added to a 100 mL round-bottom flask and stirred neat at 80 °C for 48 h. The resulting white suspension of dibutylammonium bromide was filtered through celite, and then concentrated *in vacuo*. The residue was filtered through celite directly into a 50 mL round-bottom flask and combined with 8-bromo-1-octene (7.20 g, 37.7 mmol), which were then heated to 80 °C with stirring for 72 hours. The resulting brown oil was washed with 3×25 mL portions of diethyl ether, followed by salt metathesis with excess $NaPF_6$ in deionized water The crude product was isolated as a brown oil and purified by crystallization from 1-butanol to give a white powder (1.68 g, 3.39 mmol, 14.1 % yield (on 0.5 eq. dibutylamine)). ^1H NMR (300 MHz, $CDCl_3$) δ 5.79 (ddt, *J* = 16.9, 10.1, 6.7 Hz, 2H), 5.06 – 4.89 (m, 4H), 3.14 (dt, *J* = 12.2, 3.2 Hz, 8H), 2.11 – 1.98 (m, 4H), 1.59 (qt, *J* = 7.8, 6.0 Hz, 8H), 1.50 – 1.32 (m, 16H), 0.99 (t, *J* = 7.2 Hz, 6H). $^{13}C\{^1H\}$ NMR (76 MHz, $CDCl_3$) δ 138.7, 114.7, 58.7, 58.6, 33.6, 28.6, 28.5, 26.1, 23.8, 21.9, 19.7, 13.6. ESI (+)-MS: *m/z* 350.6.

R21

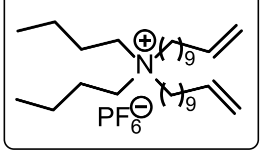

Synthesis of R21: 11-bromo-1-undecene (1.169 g, 5.013 mmol), dibutylamine (1.85 mL, 11 mmol), and potassium iodide (50 mg, 0.3 mmol, 0.06 eq.) were combined neat in a 2 dram vial and stirred at 80 °C until the mixture solidified after five days. The crude mixture was triturated with 15 mL of pentane and filtered to remove dibutylammonium bromide, and the resulting solution was concentrated in vacuo. The crude dibutylundecenylamine was added to a vial, to which was added another portion of 11-bromo-1-undecene (1.169 g, 5.013 mmol) and potassium iodide (50 mg, 0.3 mmol, 0.06 eq.), and the resulting suspension was stirred at 80 °C for one week. The mixture was then dissolved in 7 mL methanol and added to a solution of $NaPF_6$ (840 mg, 1.2 eq.) in 7 mL deionized water, forming the crude product as a brown oil, which was then dissolved in 20 mL dichloromethane. This solution was washed with 2×10 mL deionized water and 1×5 mL saturated aqueous sodium chloride, and dried with sodium sulfate. The organic layer was removed in vacuo and the crude residue recrystallized from 1-butanol to give a white powder (0.661 g, 1.14 mmol, 22.8% yield (on the first portion of 11-bromo-1-undecene)). ^1H NMR (300 MHz, $CDCl_3$) δ 5.74 (ddt, *J* = 16.9, 10.2, 6.7 Hz, 2H), 4.99 – 4.81 (m, 4H), 3.14 – 3.00 (m, 8H), 2.04 – 1.90 (m, 4H), 1.59 – 1.46 (m, 8H), 1.40 – 1.18 (m, 28H), 0.92 (t, *J* = 7.2 Hz, 6H). $^{13}C\{^1H\}$ NMR (76 MHz, $CDCl_3$) δ 139.3, 114.3, 58.7, 58.6, 33.9, 29.4, 29.2, 29.1, 29.0, 26.3, 23.8, 21.9, 19.7, 13.6. ESI (+)-MS: *m/z* 434.7.

R7'

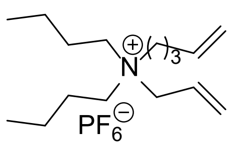

Synthesis of R7': Allyldibutylamine (77.5 mg, 0.458 mmol), 5-bromo-1-pentene (90.7 mg, 0.609 mmol) and 2 mL acetonitrile were added to a 2 dram screw-cap vial and stirred at 80 °C for 48 hours. The resulting yellow solution was combined with a solution of NaPF$_6$ (115 mg, 0.687 mmol) in 5 mL deionized water, and extracted with 3×10 mL portions of dichloromethane, which was dried with Na$_2$SO$_4$ and concentrated *in vacuo*. The crude product was isolated as a brown oil and purified by crystallization from 1-butanol to give a white powder (0.061 g, 0.16 mmol, 34.8 % yield on allyldibutylamine. ^{1}H NMR (300 MHz, CDCl$_3$) δ 5.96 – 5.49 (m, 4H), 5.12 – 4.92 (m, 2H), 3.76 (d, J = 6.9 Hz, 2H), 3.15 – 2.95 (m, 6H), 2.15 – 2.02 (m, 2H), 1.79 – 1.47 (m, 6H), 1.33 (h, J = 7.3 Hz, 4H), 0.91 (t, J = 7.3 Hz, 6H). ^{13}C NMR (126 MHz, CDCl$_3$) δ 135.57, 129.06, 123.46, 117.45, 117.40, 61.05, 58.46, 57.97, 29.88, 23.61, 20.87, 19.49, 13.47, 13.39. ESI (+)-MS: *m/z* 238.5.

R5phen

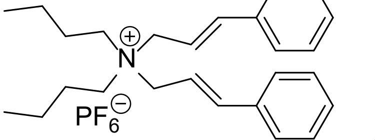

Synthesis of R5phen: Dibutylamine (136 mg, 1.05 mmol), cinnamyl bromide (425 mg, 2.16 mmol), potassium carbonate (290 mg, 2.10 mmol), and 1 mL acetonitrile are combined in a 2 dram screw-cap vial. The mixture is stirred at 80 °C for 3.5 hours, at which point the mixture had completely solidified. The resulting solid suspension was dissolved in 15 mL acetonitrile, filtered through a cotton wool plug, and concentrated *in vacuo*. The resulting yellow oil was redissolved in 3 mL methanol and combined with a solution of NaPF$_6$ (0.265 g, 1.58 mmol) in 10 mL deionized water. The resulting flocculant white precipitate is filtered, washed with 2×5 mL deionized water, and dried under high vacuum, giving the product dibutyldicinnamylammonium hexafluorophosphate as a white powder (0.375 g, 0.737 mmol, 70.2% yield on dibutylamine). ^{1}H NMR (300 MHz, d_6-DMSO) δ 7.66 – 7.57 (m, 4H), 7.46 – 7.31 (m, 6H), 6.99 (d, J = 15.6 Hz, 2H), 6.49 (dt, J = 15.2, 7.3 Hz, 2H), 4.11 (d, J = 7.3 Hz, 4H), 3.30 – 3.16 (m, 4H), 1.85 – 1.65 (m, 4H), 1.32 (h, J = 7.4 Hz, 4H), 0.93 (t, J = 7.3 Hz, 6H). ^{13}C NMR (76 MHz, d_6-DMSO) δ 140.35, 135.31, 128.88, 128.66, 127.17, 116.26, 60.01, 57.38, 23.02, 19.21, 13.44. ESI (+)-MS: *m/z* 362.6.

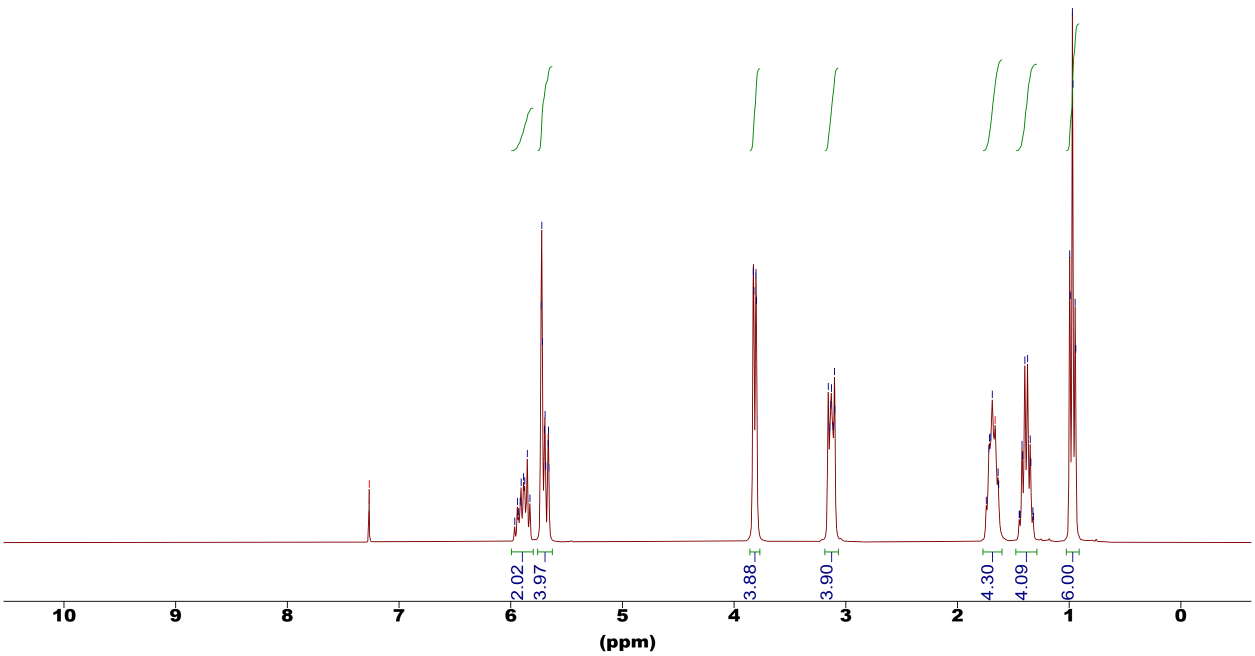

Figure S1. ^{1}H NMR spectrum of **R5**.

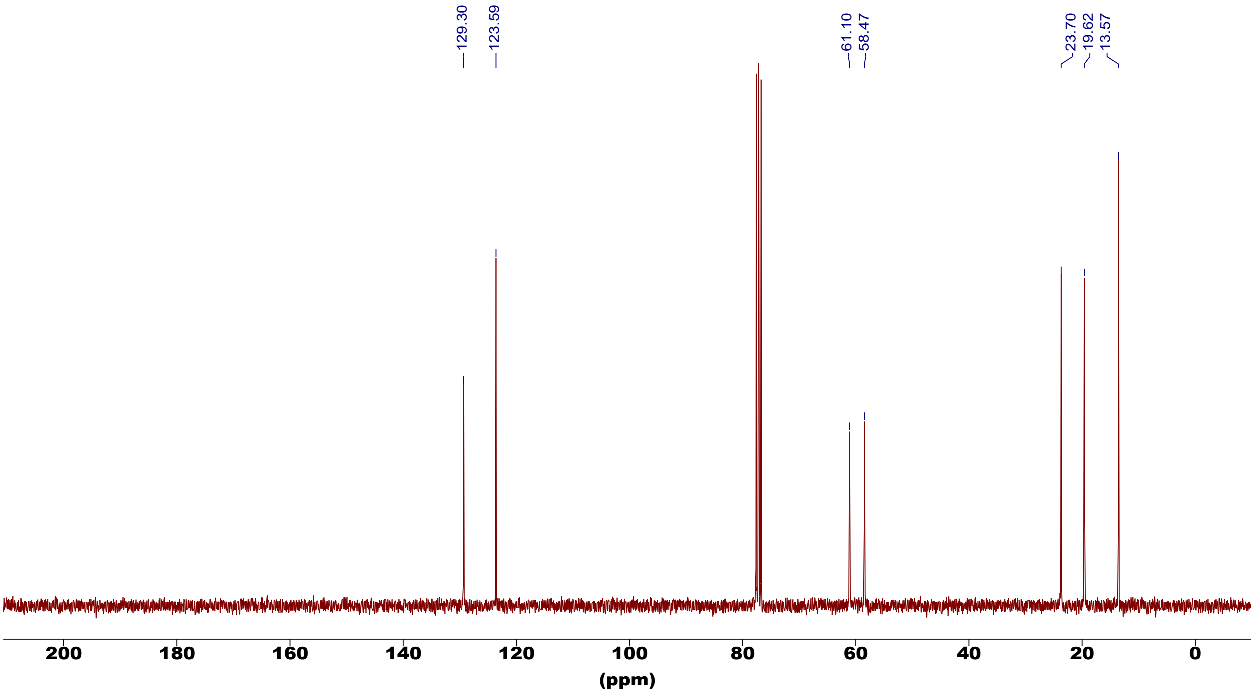

Figure S2. ^{13}C NMR spectrum of **R5**.

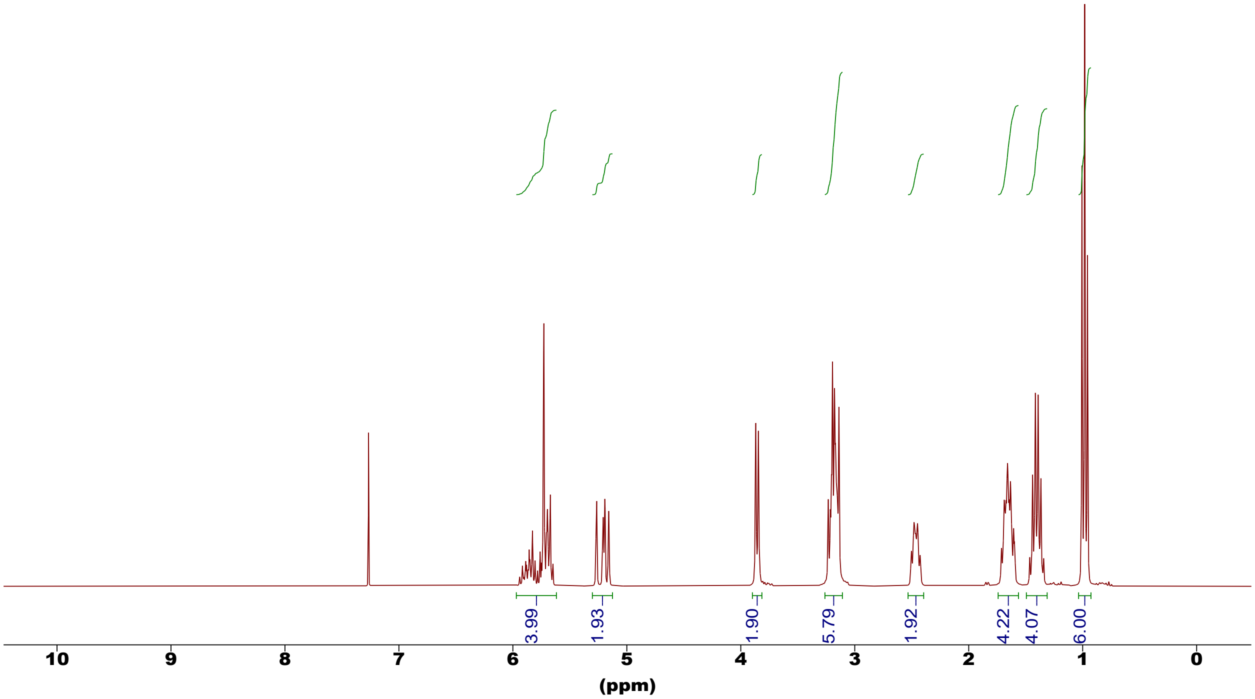

Figure S3. ^{1}H NMR spectrum of **R6**.

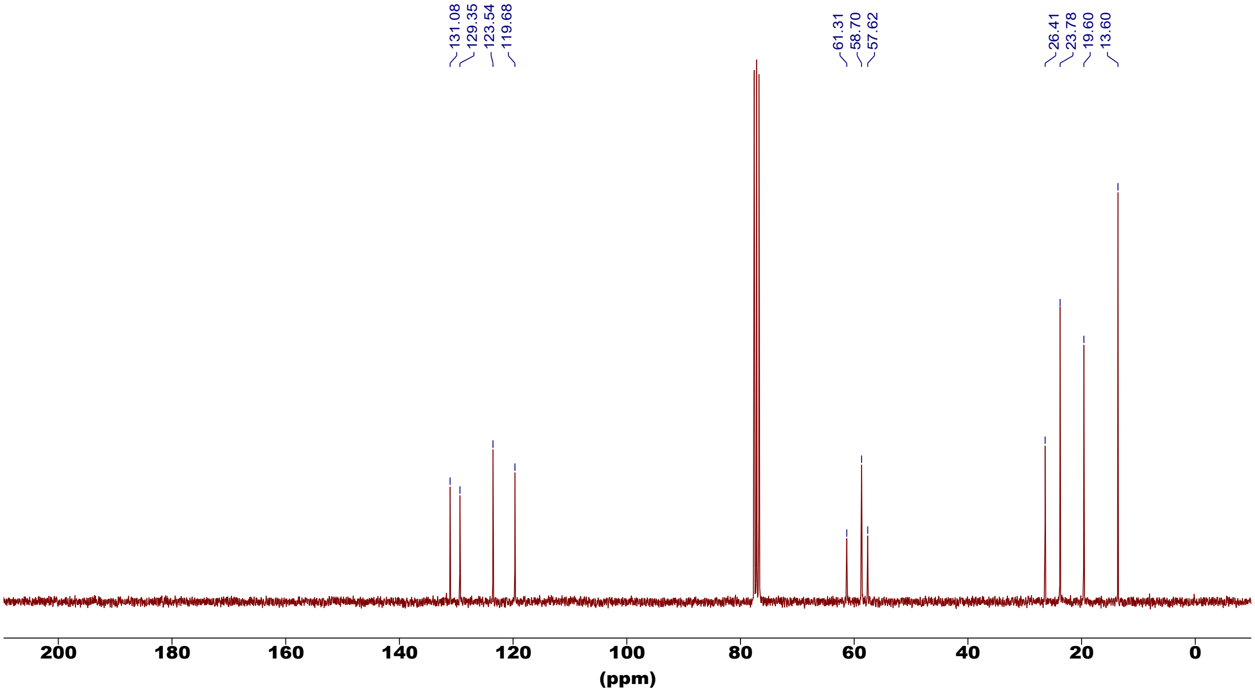

Figure S4. ^{13}C NMR spectrum of **R6**.

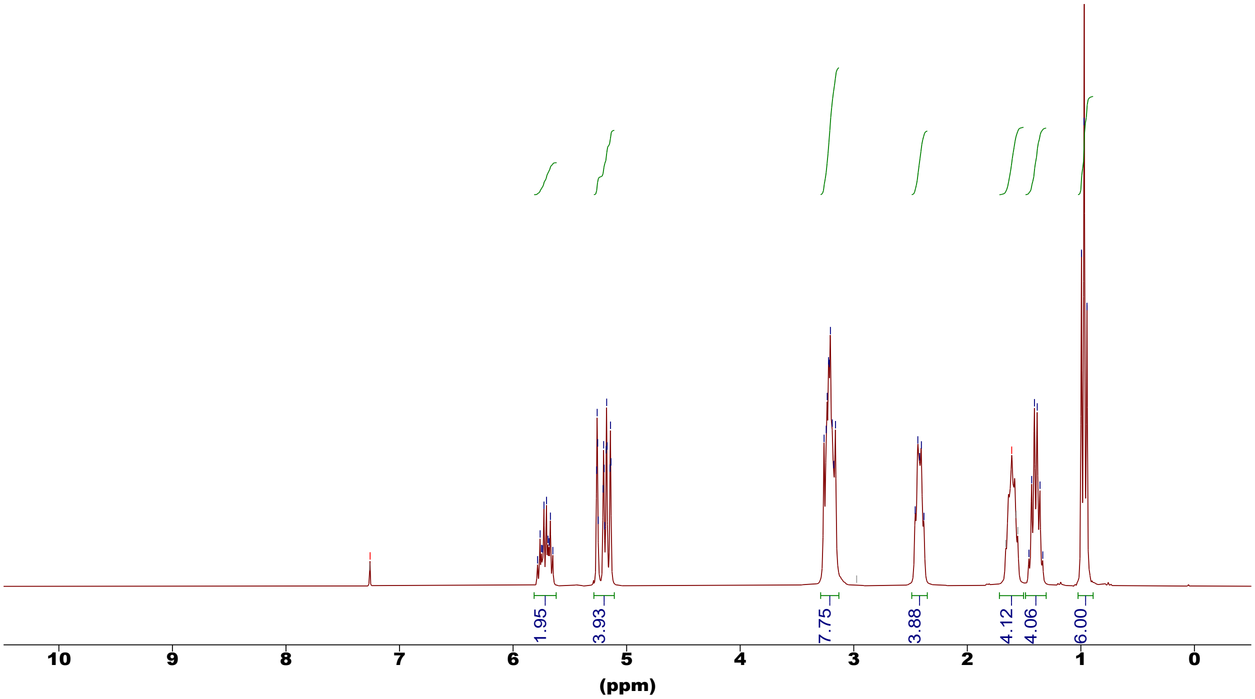

Figure S5. ^{1}H NMR spectrum of **R7**.

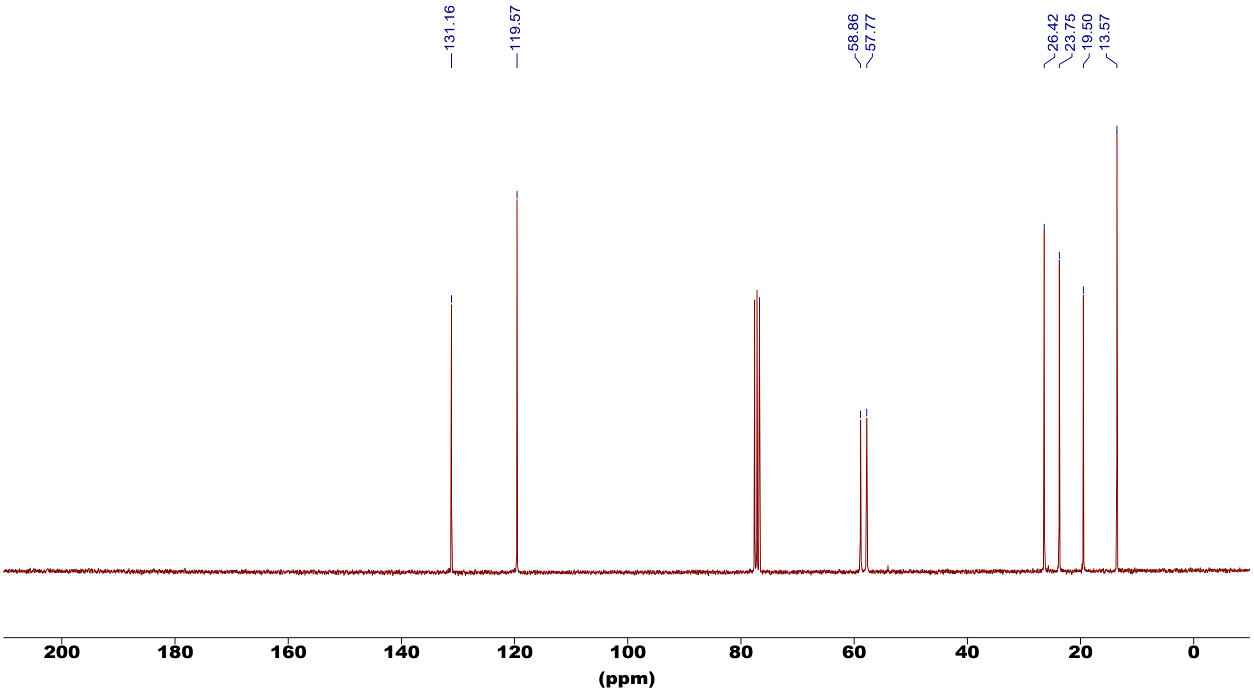

Figure S6. ^{13}C NMR spectrum of **R7**.

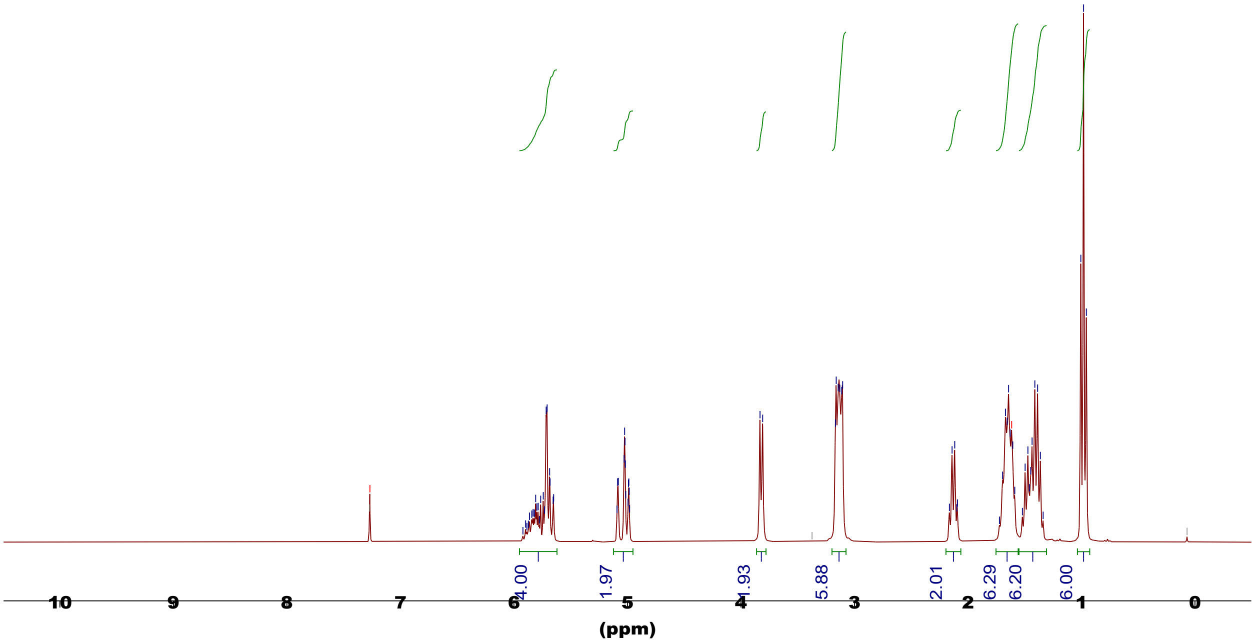

Figure S7. ^{1}H NMR spectrum of **R8**.

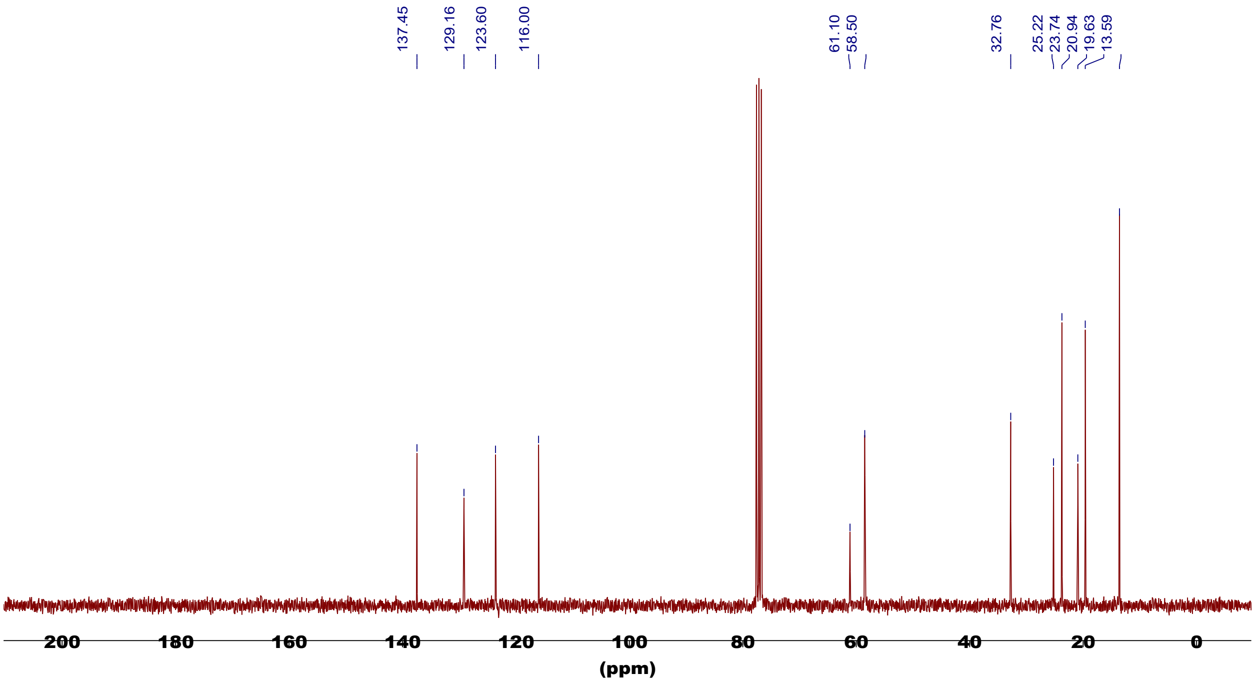

Figure S8. ^{13}C NMR spectrum of **R8**.

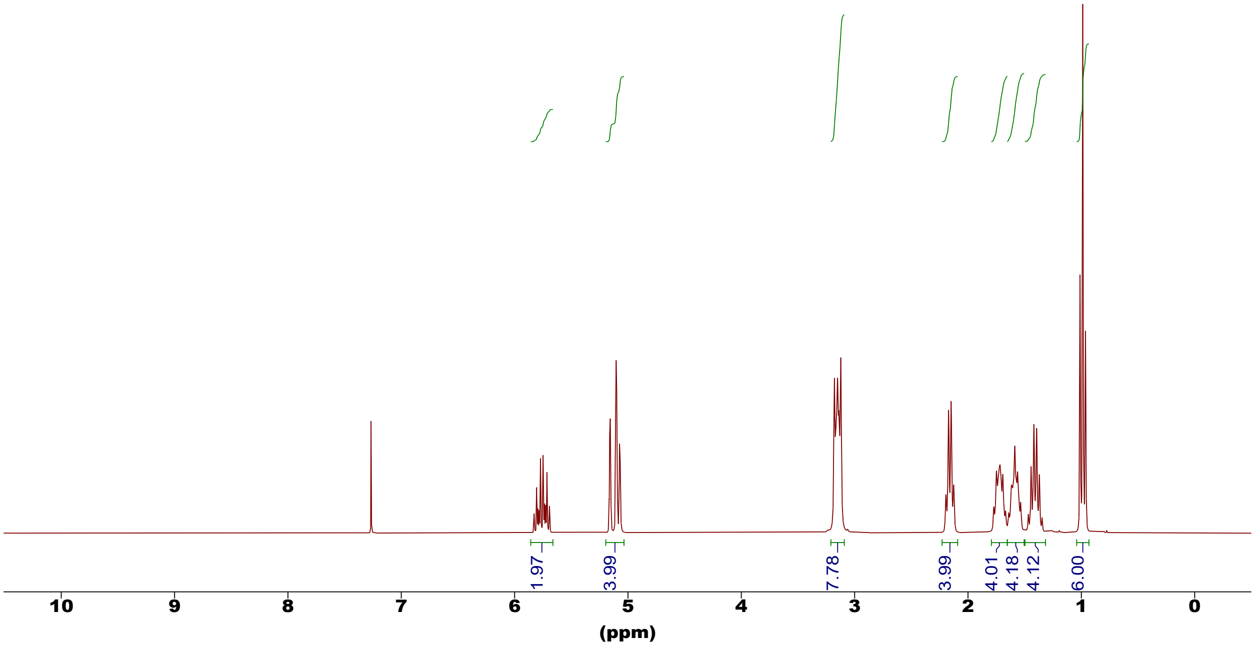

Figure S9. ^{1}H NMR spectrum of **R9**.

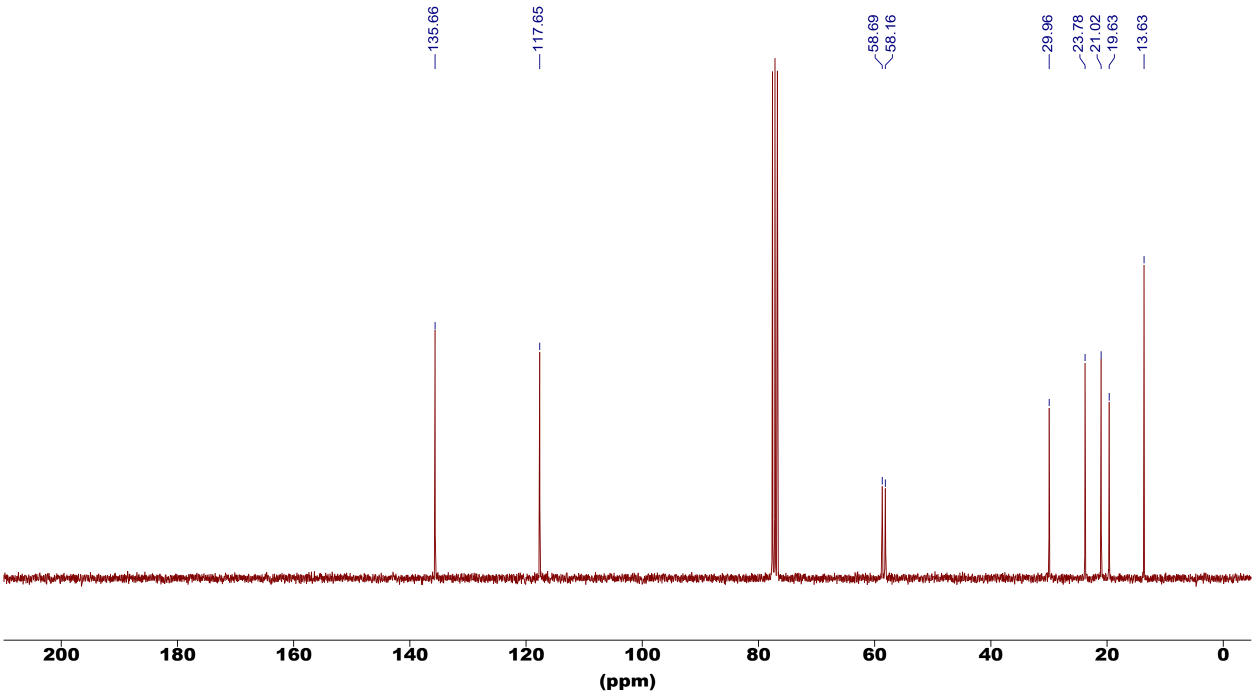

Figure S10. ^{13}C NMR spectrum of **R9**.

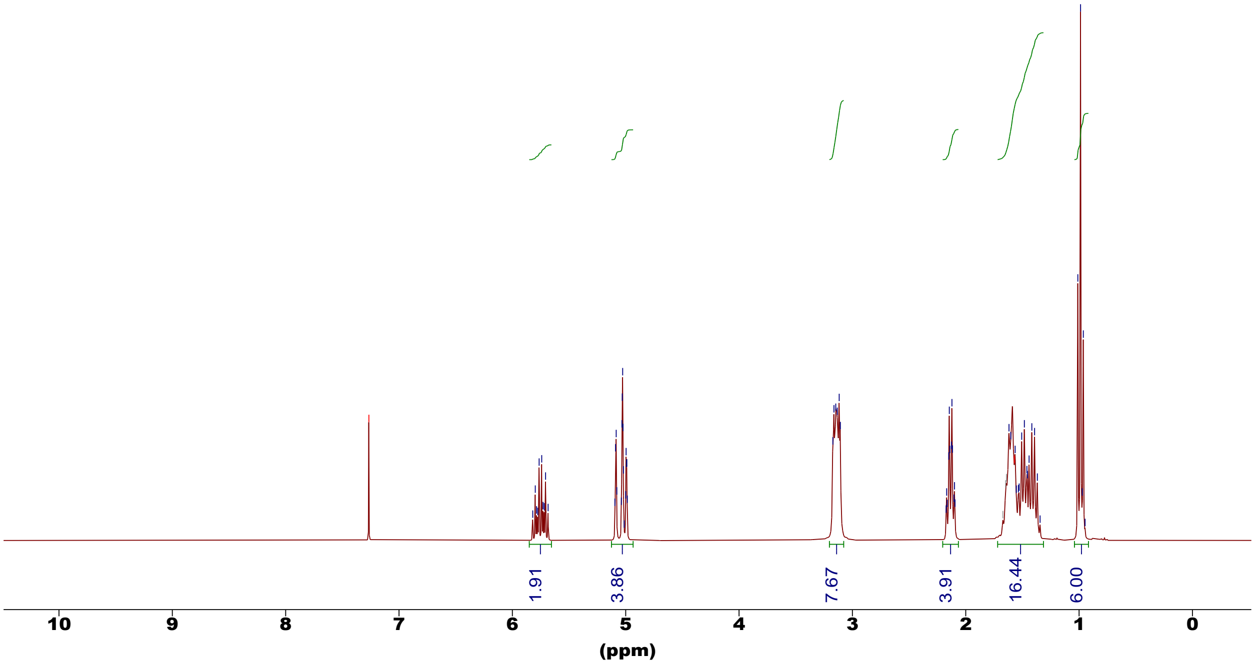

Figure S11. ^{1}H NMR spectrum of **R11**.

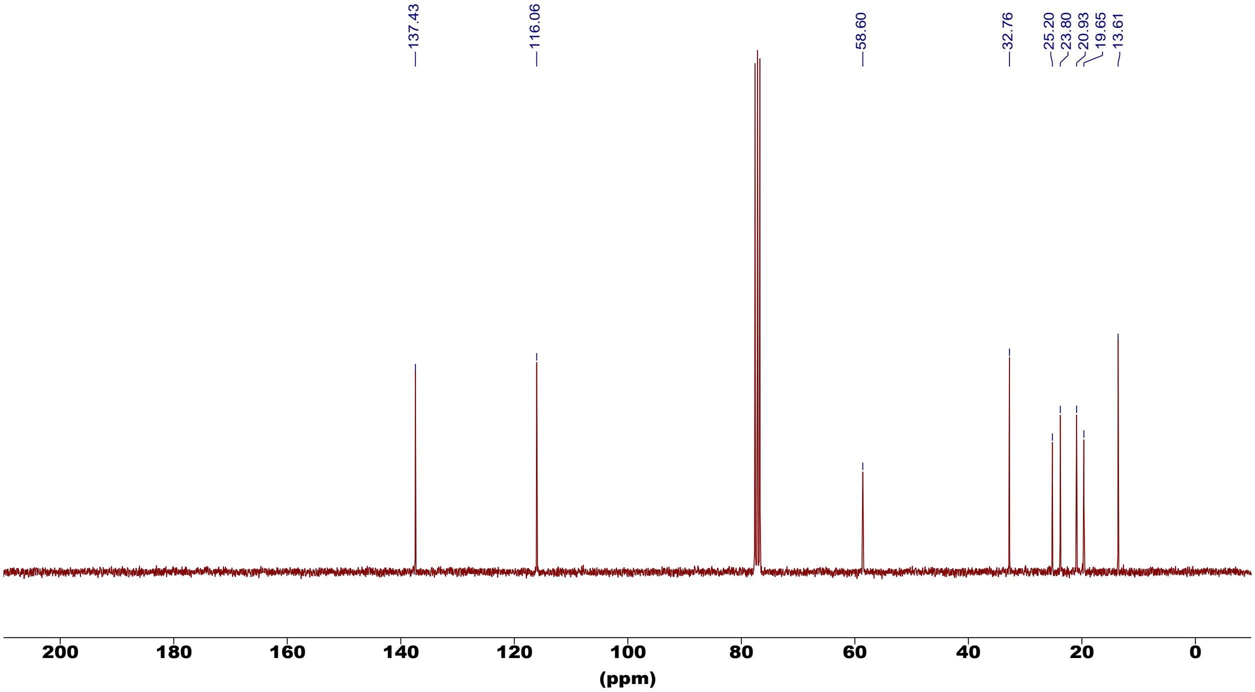

Figure S12. ^{13}C NMR spectrum of **R11**.

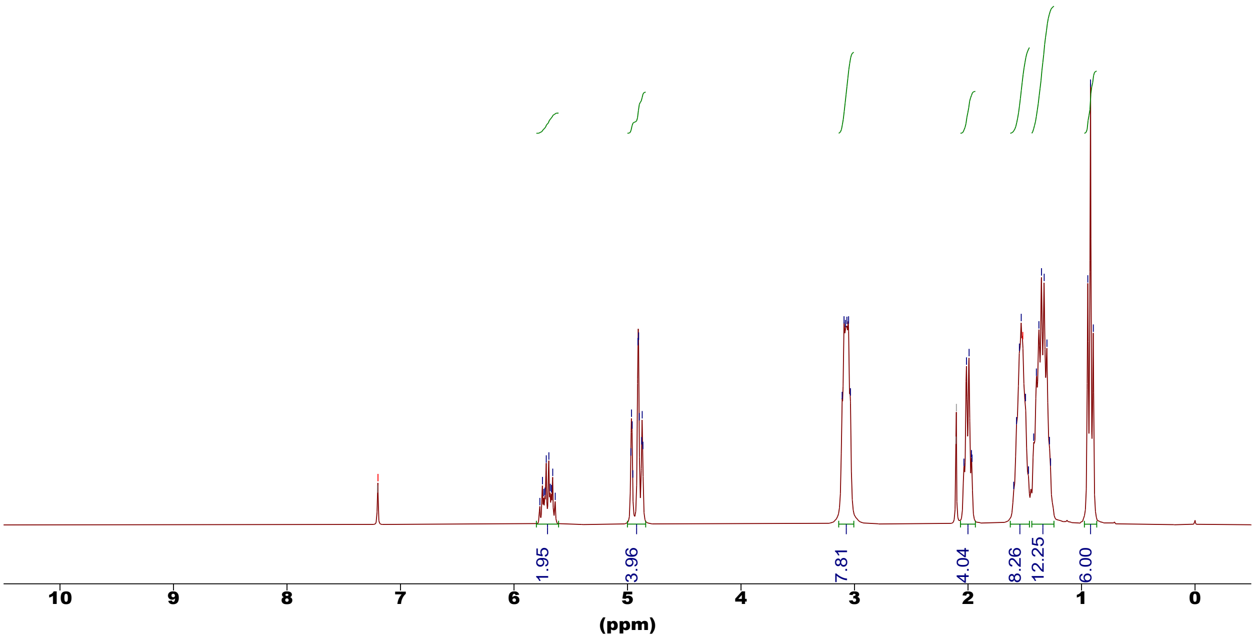

Figure S13. ^{1}H NMR spectrum of **R13**.

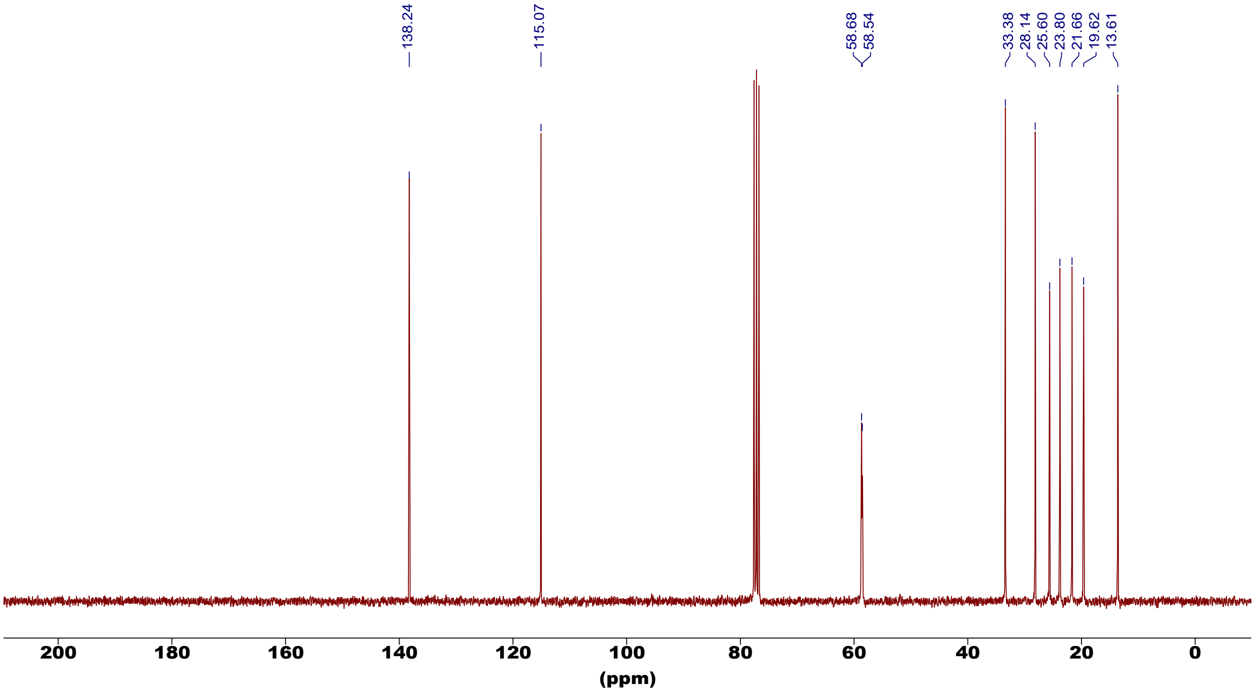

Figure S14. ^{13}C NMR spectrum of **R13**.

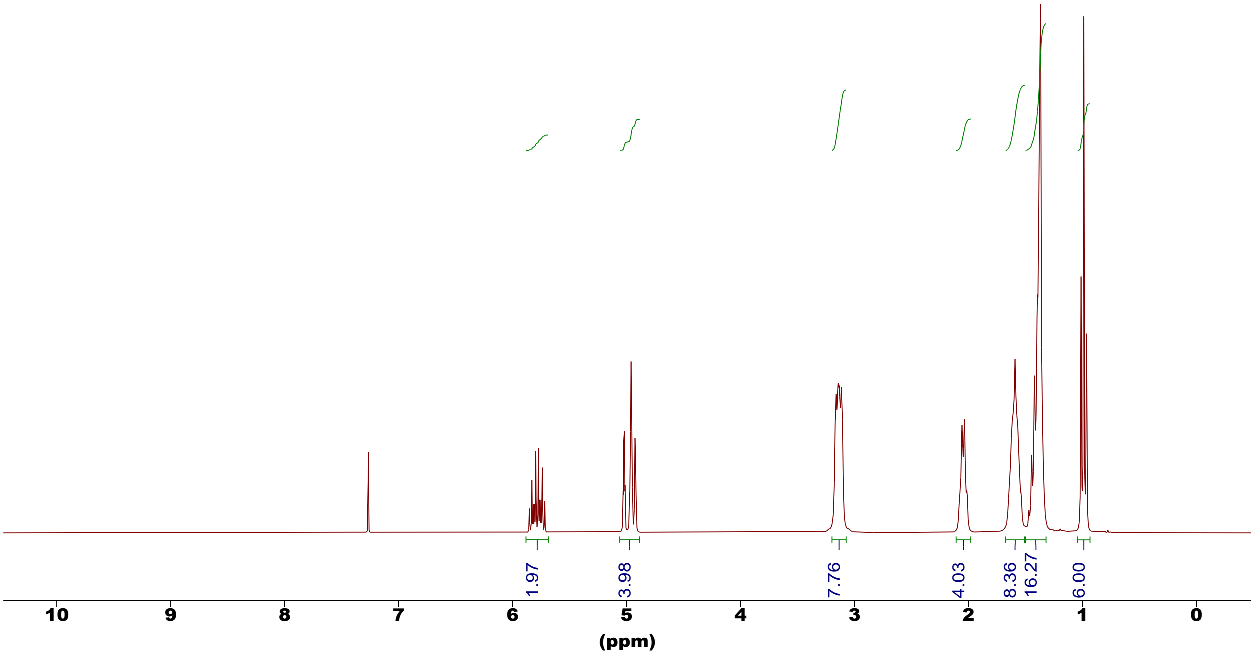

Figure S15. ^{1}H NMR spectrum of **R15**.

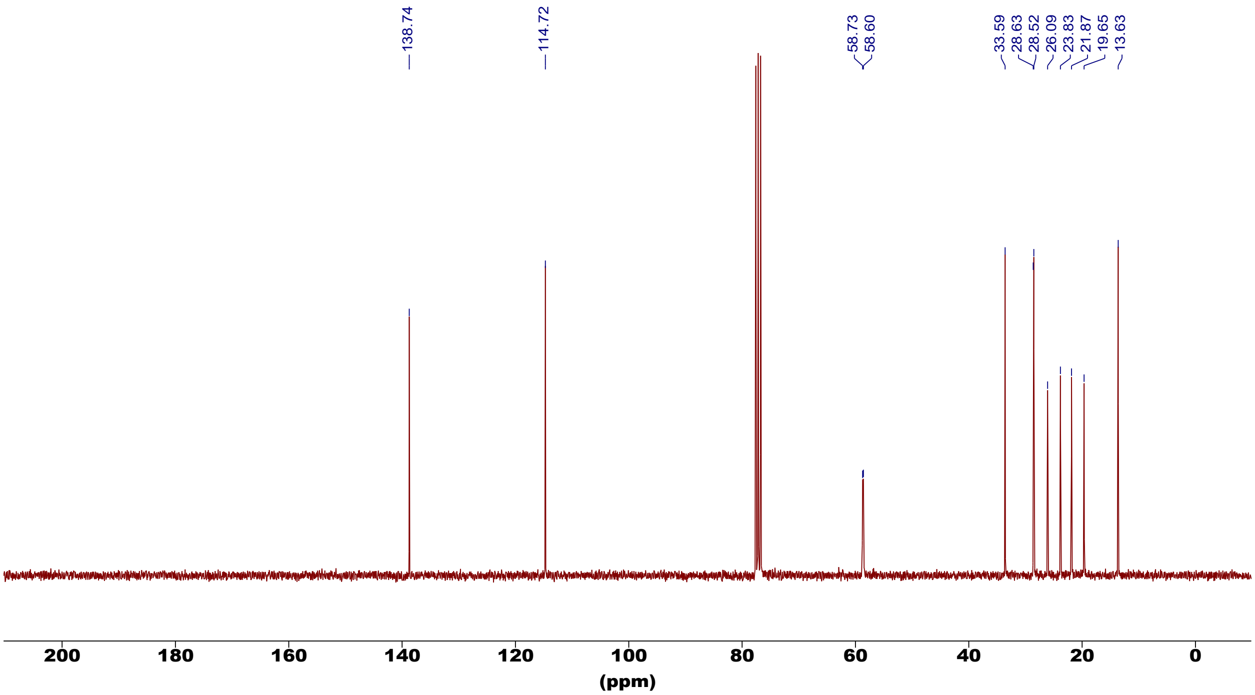

Figure S16. ^{13}C NMR spectrum of **R15**.

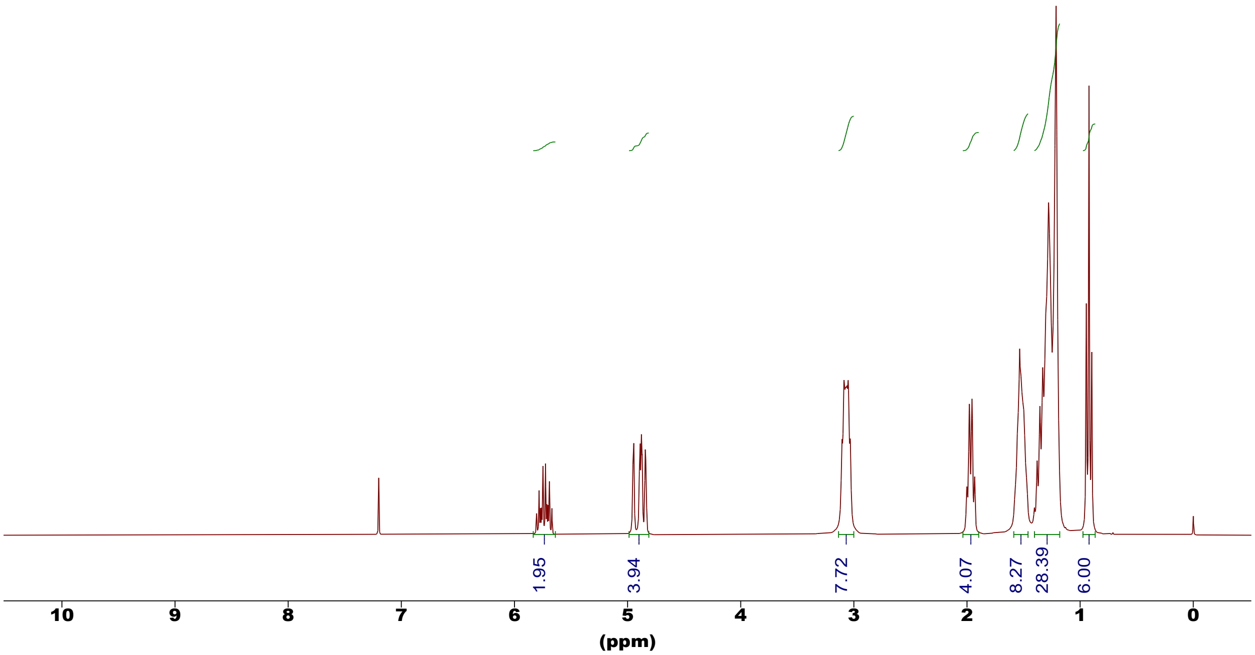

Figure S17. ^{1}H NMR spectrum of **R21**.

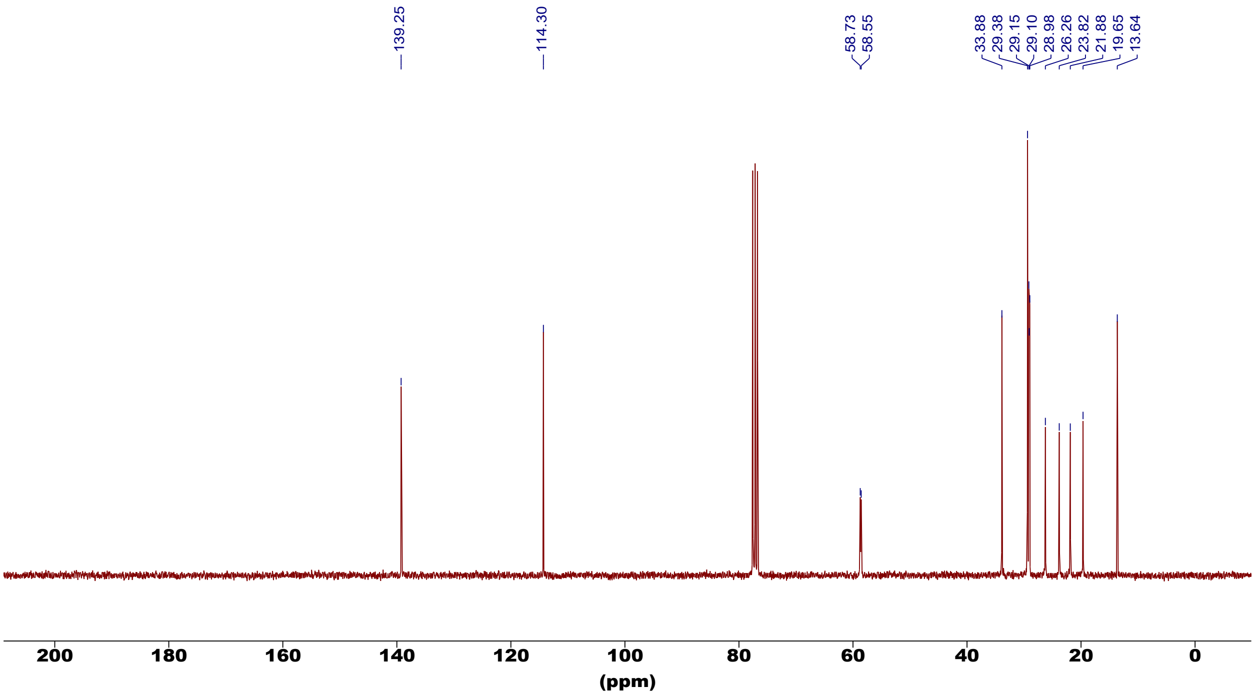

Figure S18. ^{13}C NMR spectrum of **R21**.

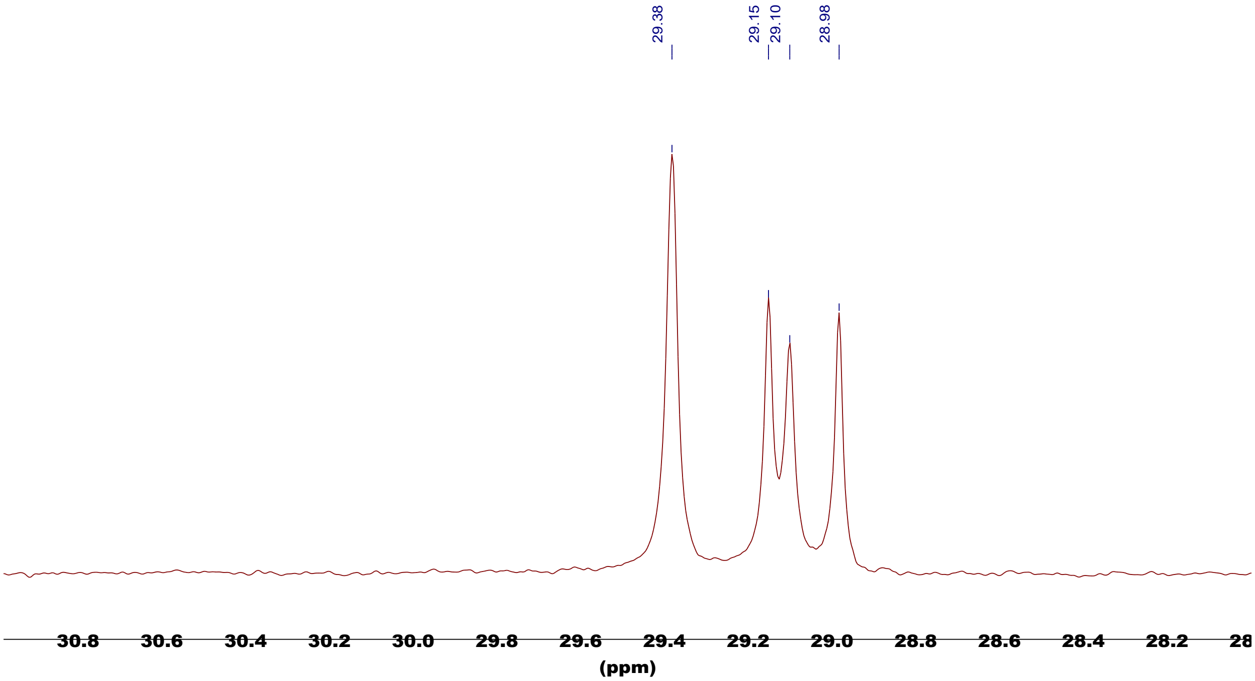

Figure S19. ^{13}C NMR spectrum of **R21** between 28-31 ppm.

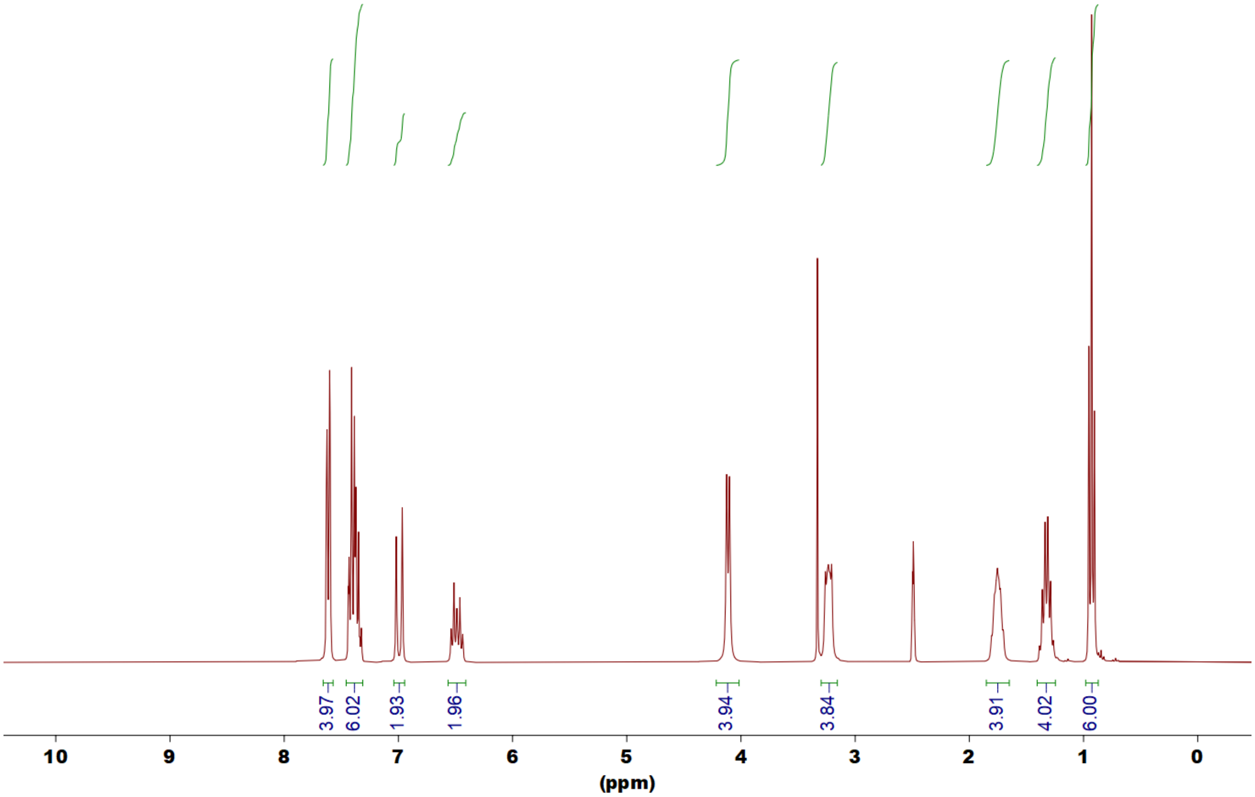

Figure S20. ^{1}H NMR spectrum of **R5-phen**.

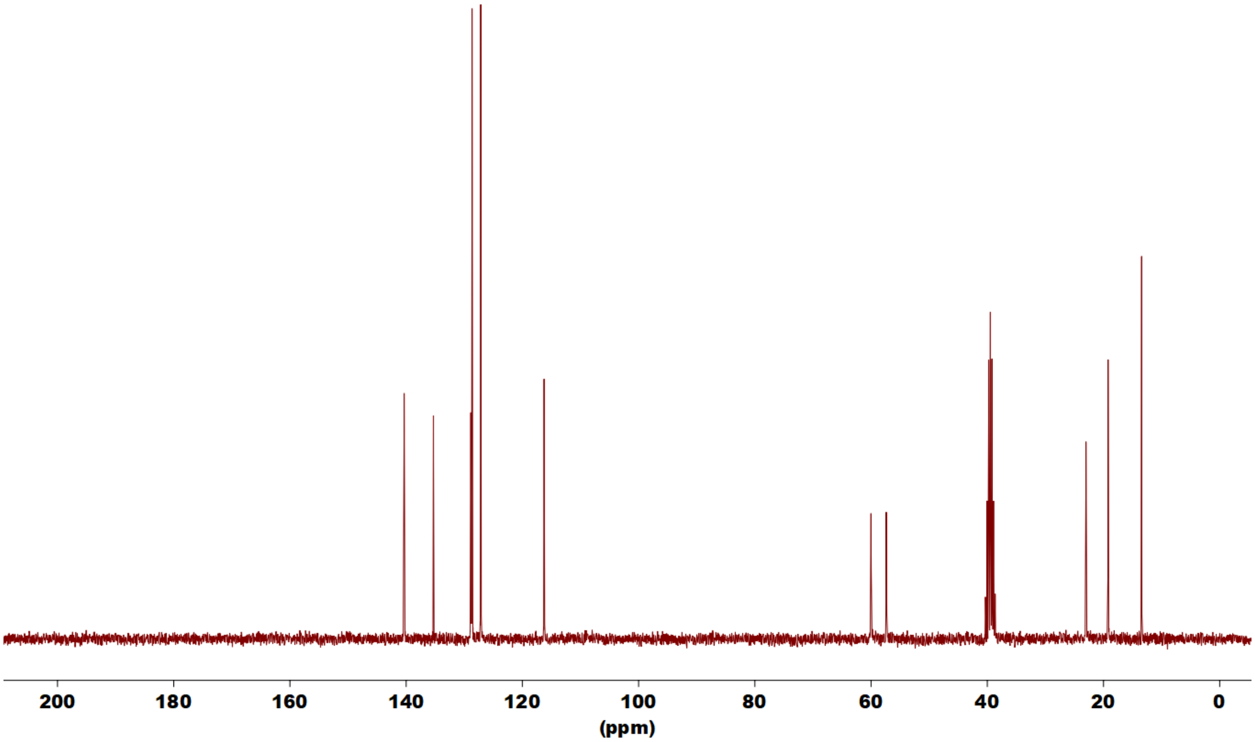

Figure S21. ^{13}C NMR spectrum of **R5-phen**.

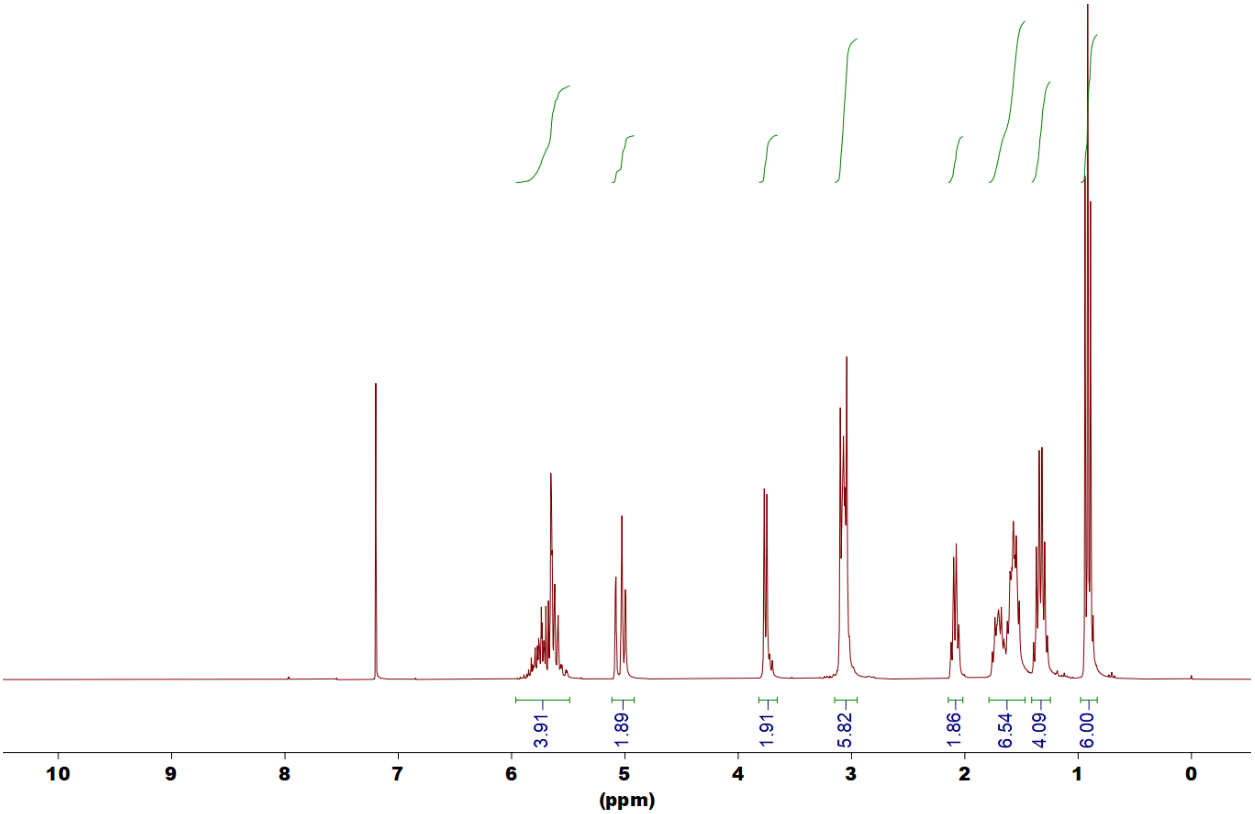

Figure S22. ^{1}H NMR spectrum of **R7'**.

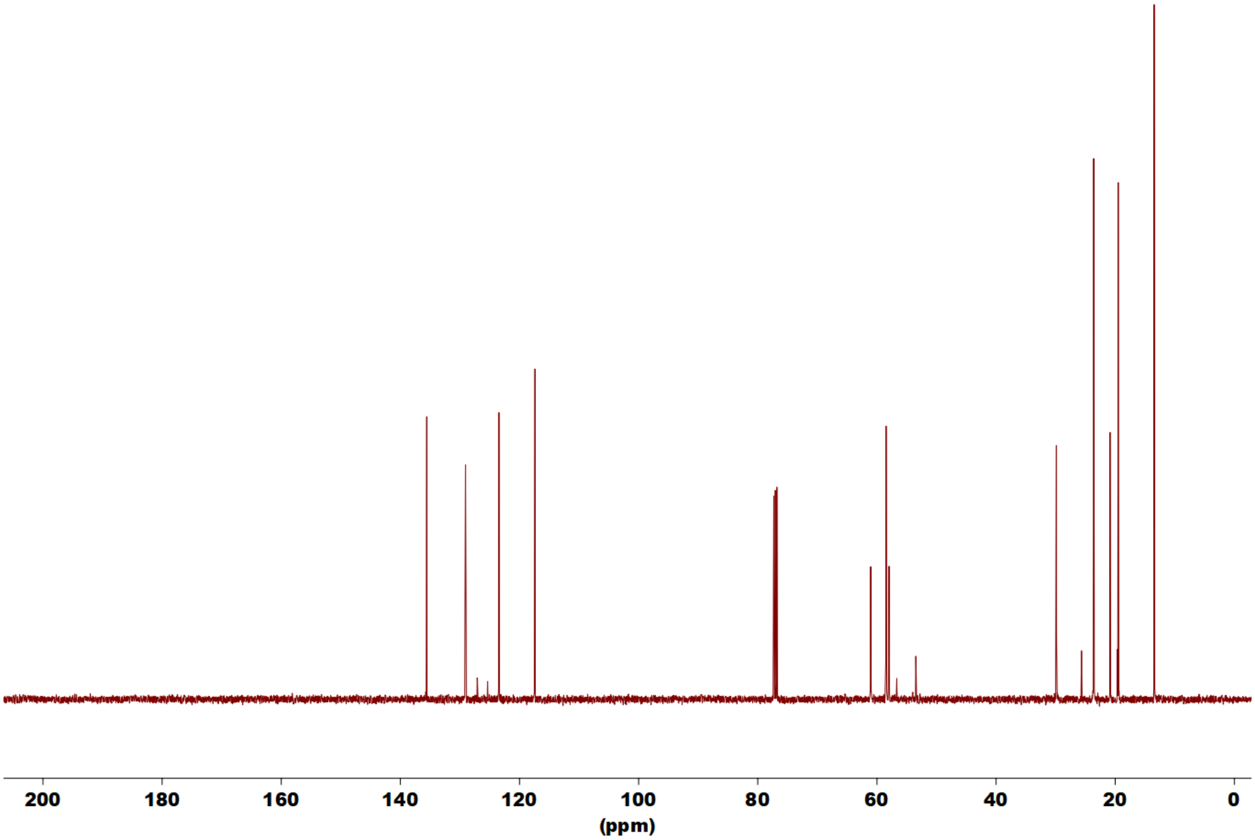

Figure S23. ^{13}C NMR spectrum of **R7’**.

Table T1. Kinetic data from each individual competition experiment, showing rates of substrate consumption relative to that of the rate of **R21**.

Expt/Sub	1	2	3	4	5	6	7	8	9	10	Avg. k (/R21)	Std. Error
R5		0.035							0.119	0.053	0.069	0.026
R6	0.444	0.345		0.363							0.384	0.030
R7	0.766			0.707		0.787	0.737				0.749	0.017
R8			0.731		0.556			0.532			0.607	0.063
R9			0.505					0.513	0.603		0.540	0.031
R11					0.809	0.853	0.874			0.775	0.828	0.022
R13	1.103	0.982	1.168	1.018							1.068	0.042
R15					1.102	1.129	1.154	1.077	1.104	1.114	1.113	0.011
R21	1	1	1	1	1	1	1	1	1	1	1.000	x

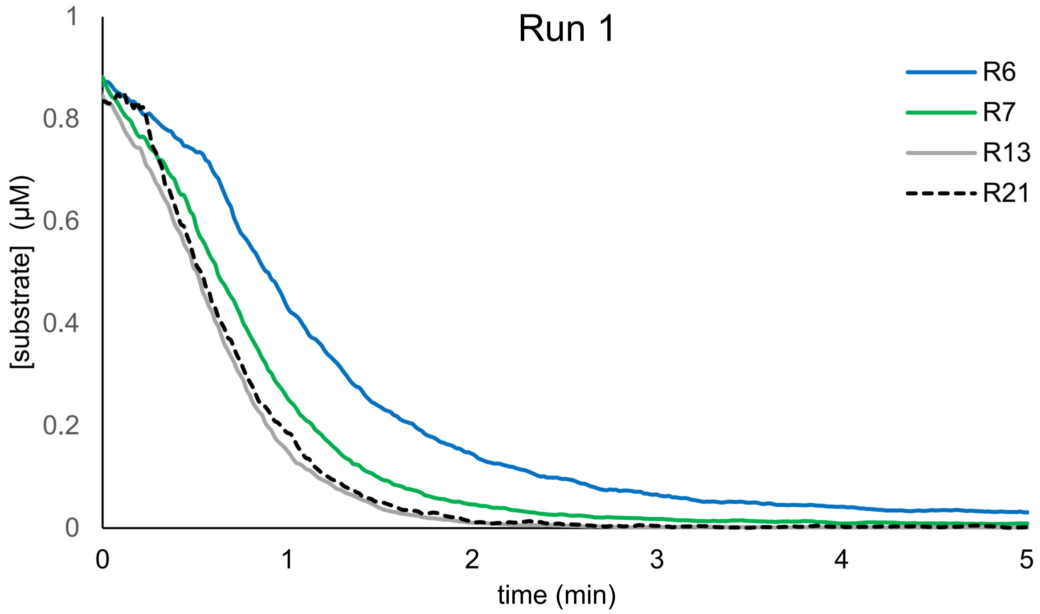

Figure S24. Kinetic data from Run 1, shown as a rolling average of 10 data points. Substrate concentration in micromolar is shown on the y-axis, with time shown in minutes on the x-axis.

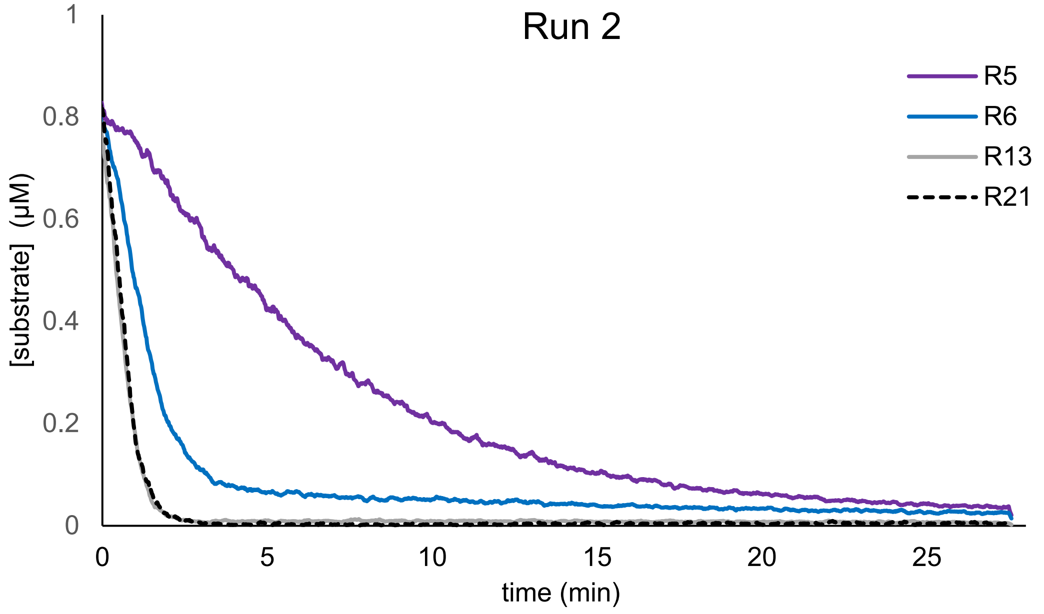

Figure S25. Kinetic data from Run 2, shown as a rolling average of 10 data points. Substrate concentration in micromolar is shown on the y-axis, with time shown in minutes on the x-axis.

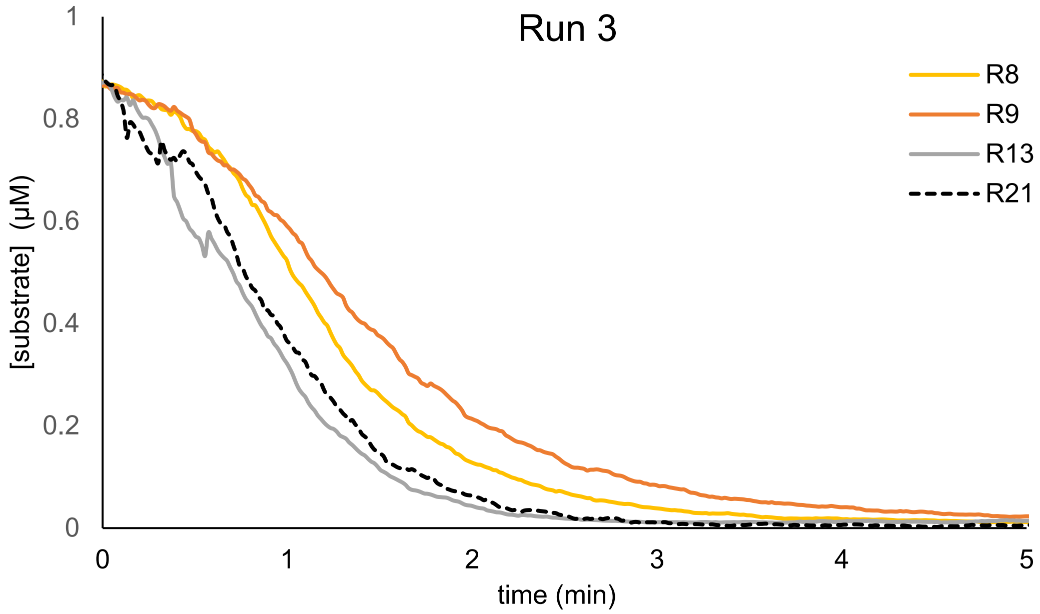

Figure S26. Kinetic data from Run 3, shown as a rolling average of 10 data points. Substrate concentration in micromolar is shown on the y-axis, with time shown in minutes on the x-axis.

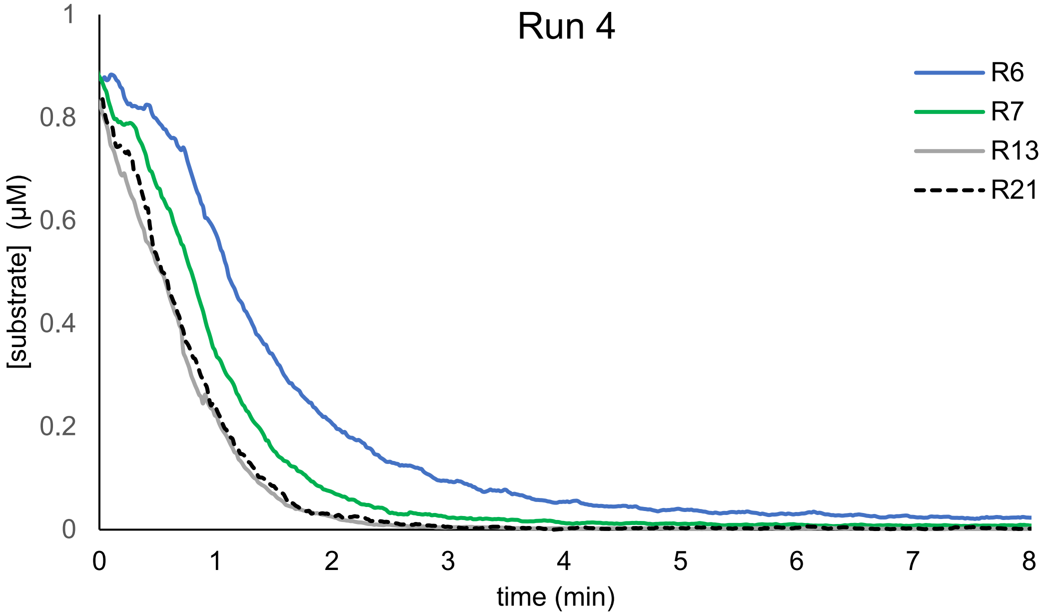

Figure S27. Kinetic data from Run 4, shown as a rolling average of 10 data points. Substrate concentration in micromolar is shown on the y-axis, with time shown in minutes on the x-axis.

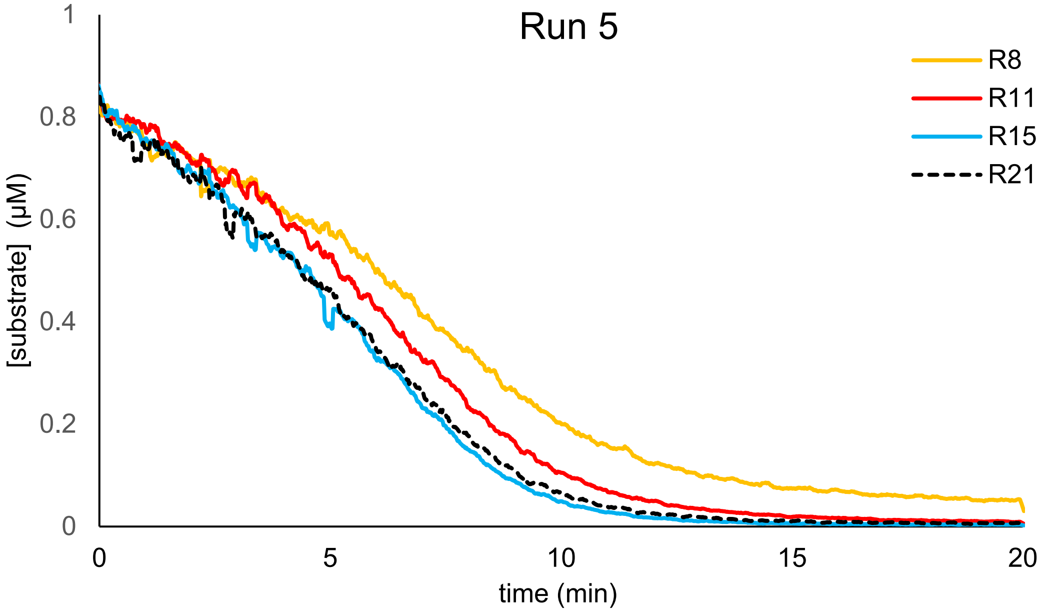

Figure S28. Kinetic data from Run 5, shown as a rolling average of 10 data points. Substrate concentration in micromolar is shown on the y-axis, with time shown in minutes on the x-axis.

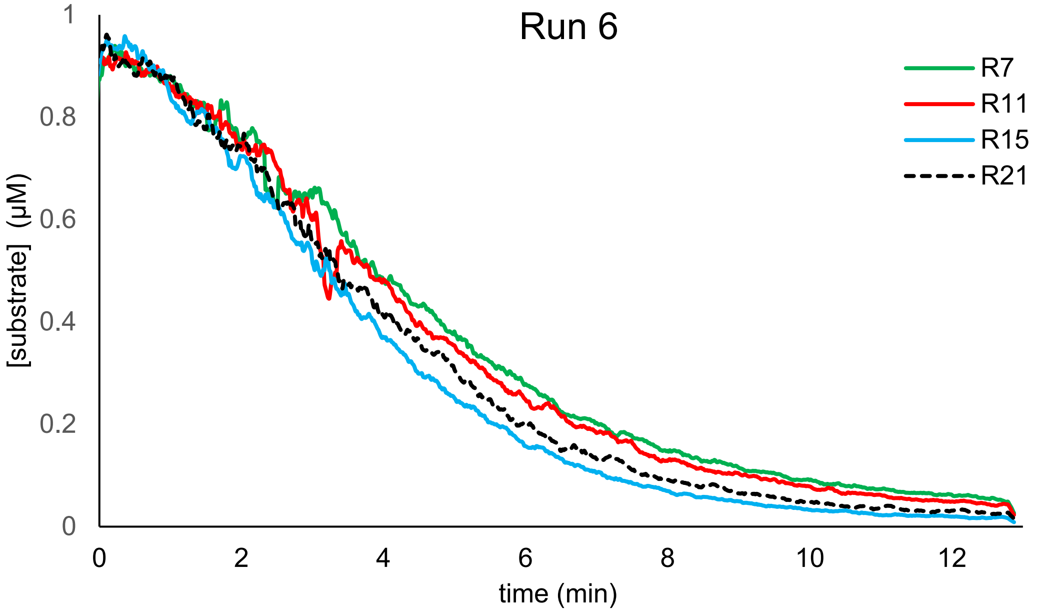

Figure S29. Kinetic data from Run 6, shown as a rolling average of 10 data points. Substrate concentration in micromolar is shown on the y-axis, with time shown in minutes on the x-axis.

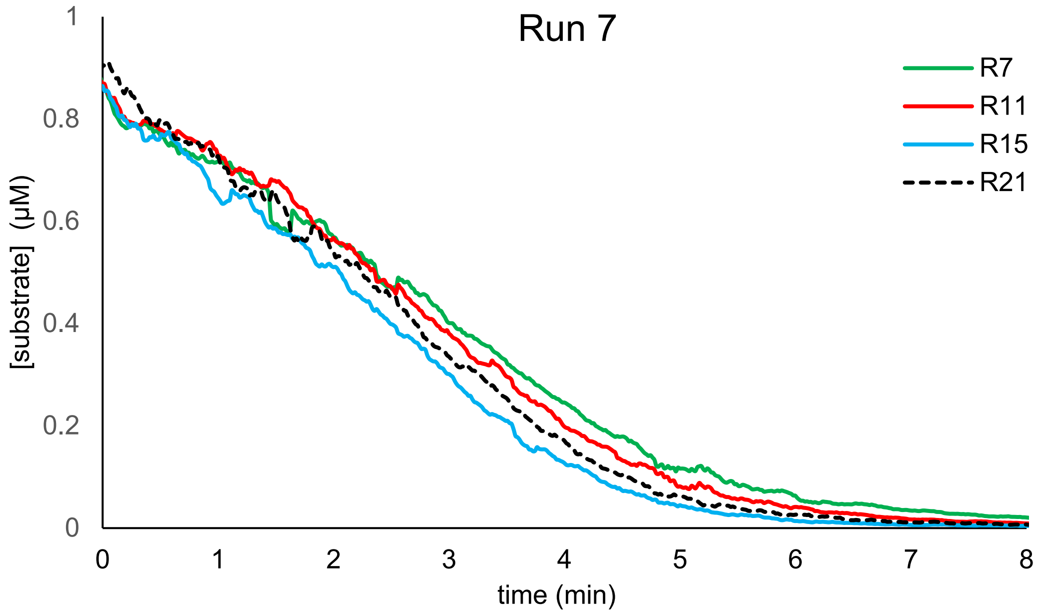

Figure S30. Kinetic data from Run 7, shown as a rolling average of 10 data points. Substrate concentration in micromolar is shown on the y-axis, with time shown in minutes on the x-axis.

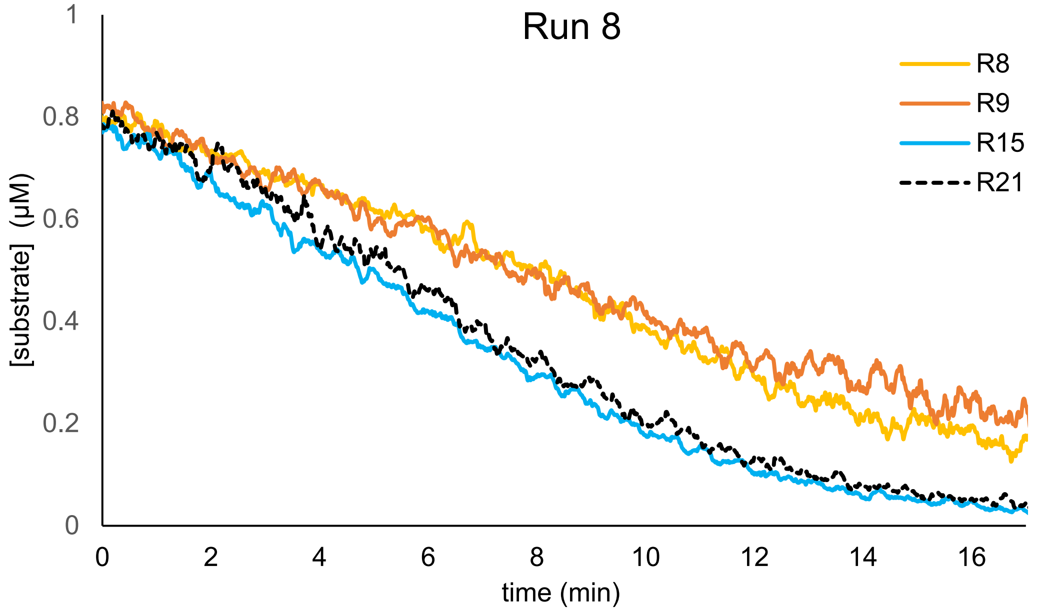

Figure S31. Kinetic data from Run 8, shown as a rolling average of 10 data points. Substrate concentration in micromolar is shown on the y-axis, with time shown in minutes on the x-axis.

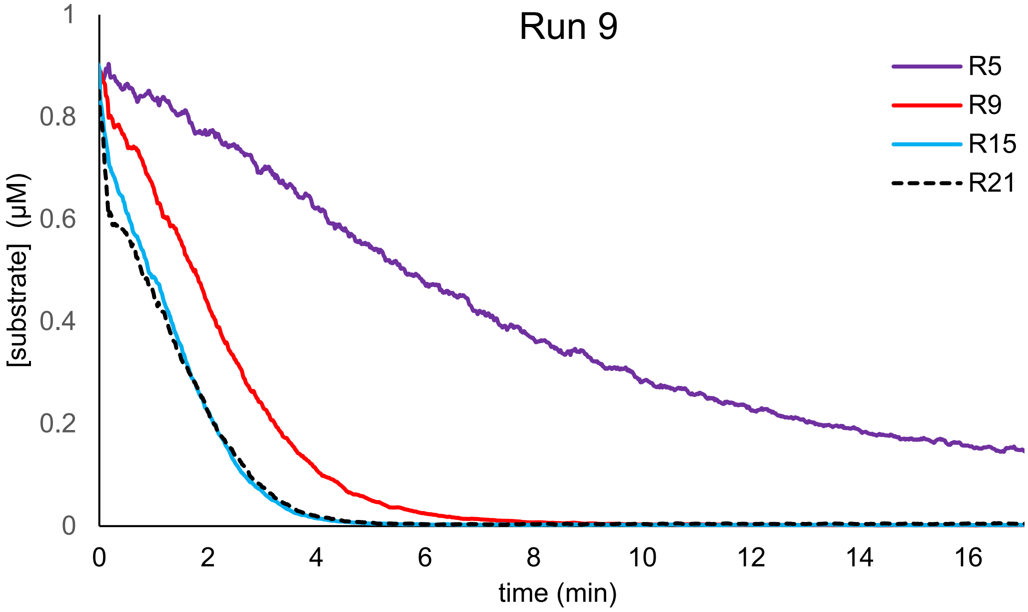

Figure S32. Kinetic data from Run 9, shown as a rolling average of 10 data points. Substrate concentration in micromolar is shown on the y-axis, with time shown in minutes on the x-axis.

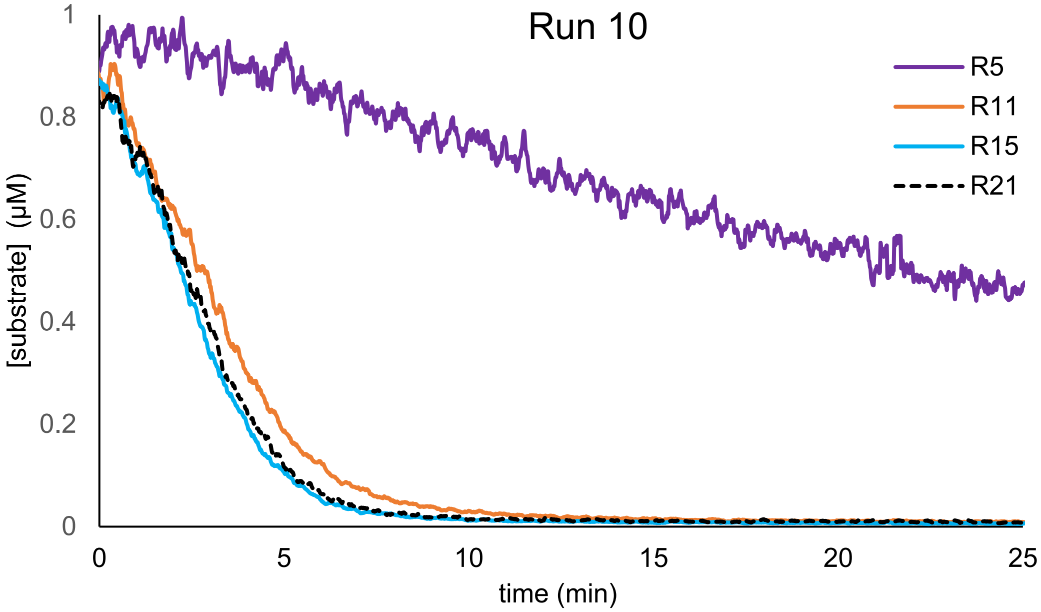

Figure S33. Kinetic data from Run 10, shown as a rolling average of 10 data points. Substrate concentration in micromolar is shown on the y-axis, with time shown in minutes on the x-axis.

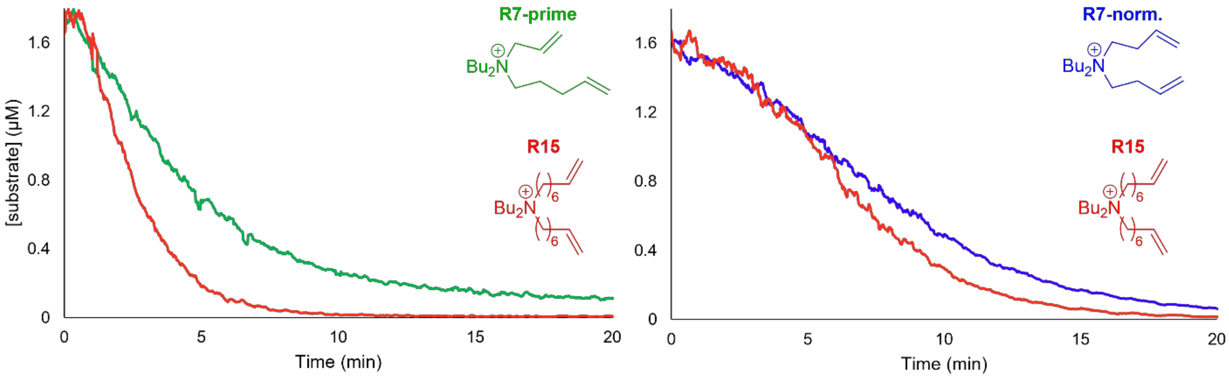

Figure S34. Rates of RCM of asymmetric **R7’** (left, green) and symmetric **R7** (right, blue), compared to **R15** as an internal standard shown in red. This graph shows that the relative rate of RCM for the asymmetric **R7’** substrate when compared to the rate of **R15** in the same experiment is considerably slower than its symmetric **R7** counterpart compared to **R15**. Here, relative rates are compared instead of absolute rates due to natural variations in overall rate of RCM due to the levels of adventitious water and moisture present at 3.5 μM total catalyst concentration.

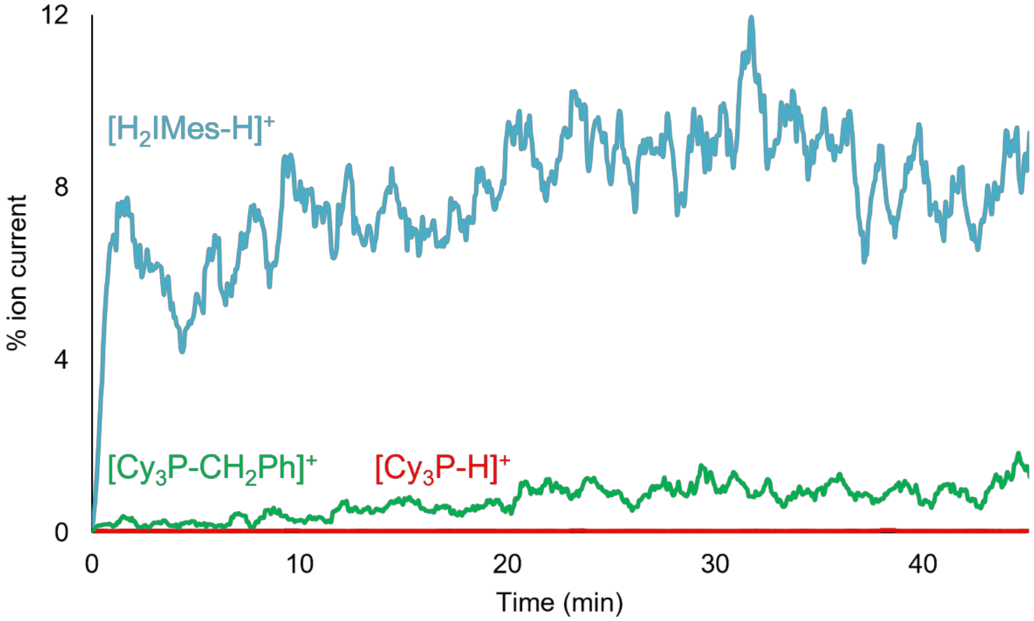

Figure S35. PSI-ESI-MS spectrum of **GII** in dichloromethane over time, with catalyst solution being added to the PSI flask at time zero. The green line shows the slow formation of the benzyltriphenylphosphonium ion, the light blue line shows the preexistence of the $[H_2IMes\text{-}H]^+$ ion in the catalyst sample, and the red line indicates the lack of formation of the $[Cy_3P\text{-}H]^+$ ion without the RCM reaction occuring.

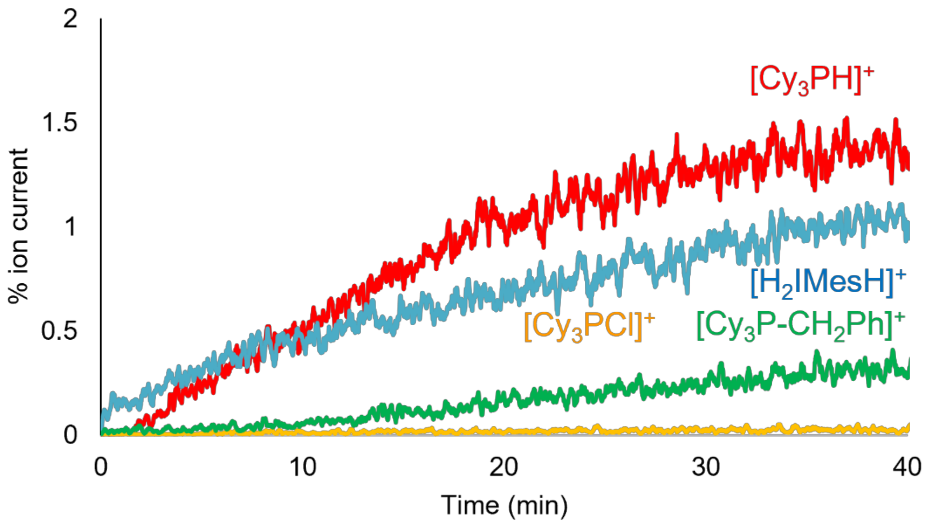

Figure S36. PSI-ESI-MS spectrum of a mixture of **GII** and the RCM-inert **R5phen** substrate, showing the formation of the typical suite of catalyst decomposition products despite no RCM occurring.

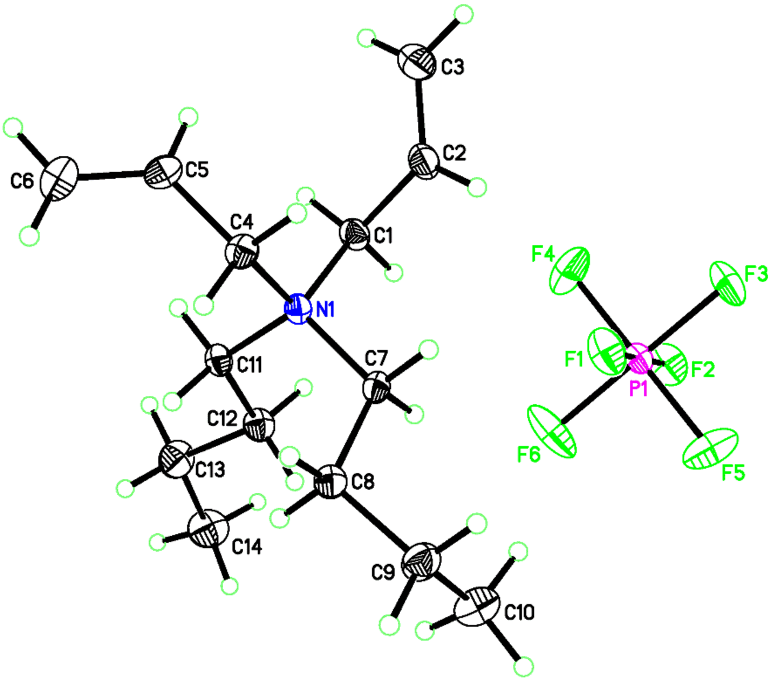

Figure S37. X-ray crystal structure of **R5**.

<u>DISCUSSION:</u>

The compound crystallizes as colorless block-like crystals from an ethanol solution. There are four molecules of the di-butyl, di-propylene ammonium cation and associated PF_6 anion in the unit cell of the primitive, centrosymmetric, monoclinic space group $P2_1/c$.

The structures of the two molecules are as expected (see Figures). Bond distances and angles are otherwise unexceptional.

<u>CRYSTAL SUMMARY:</u>

Crystal data for $C_{14}H_{28}F_6NP$; M_r = 355.34; Monoclinic; space group $P2_1/c$; a = 9.4663(13) Å; b = 13.2301(18) Å; c = 14.178(2) Å; α = 90°; β = 93.998(2)°; γ = 90°; V = 1771.4(4) Å^3; Z = 4; T = 120(2) K; λ(Mo-Kα) = 0.71073 Å; μ(Mo-Kα) = 0.207 mm^{-1}; d_{calc} = 1.332g.cm^{-3}; 41285 reflections collected; 4431 unique (R_{int} = 0.0332); giving R_1 = 0.0331, wR_2 = 0.0844 for 3751 data with [I>2σ(I)] and R_1 = 0.0417, wR_2 = 0.0890 for all 4431 data. Residual electron density (e$^-$.Å^{-3}) max/min: 0.686/-0.277.

An arbitrary sphere of data were collected on a colorless block-like crystal, having approximate dimensions of 0.198 × 0.196 × 0.108 mm, on a Bruker APEX-II diffractometer using a combination of ω- and φ-scans of 0.5°.[2] Data were corrected for absorption and polarization effects and analyzed for space group determination. The structure was solved by intrinsic phasing methods and expanded routinely.[3] The model was refined by full-matrix least-squares analysis of F^2 against all reflections.[4] All non-hydrogen atoms were refined with anisotropic atomic displacement parameters. Unless otherwise noted, hydrogen atoms were included in calculated positions. Atomic displacement parameters for the hydrogens were tied to the equivalent isotropic displacement parameter of the atom to which they are bonded (U_{iso}(H) = 1.5U_{eq}(C) for methyl, 1.2U_{eq}(C) for all others).

Table T2. Crystal data and structure refinement for uvic1601.

Identification code	uvic1601	
Empirical formula	$C_{14}H_{28}F_6NP$	
Formula weight	355.34	
Temperature	120(2) K	
Wavelength	0.71073 Å	
Crystal system	Monoclinic	
Space group	$P2_1/c$	
Unit cell dimensions	a = 9.4663(13) Å	α = 90°
	b = 13.2301(18) Å	β = 93.998(2)°
	c = 14.178(2) Å	γ = 90°
Volume	1771.4(4) Å^3	
Z	4	
Density (calculated)	1.332 g.cm^{-3}	
Absorption coefficient (μ)	0.207 mm^{-1}	
F(000)	752	
Crystal color, habit	colorless, block	
Crystal size	0.198 × 0.196 × 0.108 mm^3	
θ range for data collection	2.108 to 28.370°	
Index ranges	-12 ≤ h ≤ 12, -17 ≤ k ≤ 17, -18 ≤ l ≤ 18	
Reflections collected	41285	
Independent reflections	4431 [R_{int} = 0.0332]	
Completeness to θ = 25.242°	100.0 %	
Absorption correction	Numerical	
Max. and min. transmission	1.0000 and 0.9382	
Refinement method	Full-matrix least-squares on F^2	
Data / restraints / parameters	4431 / 0 / 201	
Goodness-of-fit on F^2	1.045	
Final R indices [I>2σ(I)]	R_1 = 0.0331, wR_2 = 0.0844	
R indices (all data)	R_1 = 0.0417, wR_2 = 0.0890	
Extinction coefficient	n/a	
Largest diff. peak and hole	0.686 and -0.277 e$^-$.Å^{-3}	

Table T3. Atomic coordinates and equivalent isotropic displacement parameters (Å^2) for uvic1601. U(eq) is defined as one third of the trace of the orthogonalized U_{ij} tensor.

	x	y	z	U(eq)
N(1)	0.74964(10)	0.39789(7)	0.83079(7)	0.015(1)
C(1)	0.61674(12)	0.33267(9)	0.81847(9)	0.018(1)
C(2)	0.55585(13)	0.30466(10)	0.90948(9)	0.022(1)
C(3)	0.53151(16)	0.20992(11)	0.93216(11)	0.030(1)
C(4)	0.85630(13)	0.35118(9)	0.90363(8)	0.018(1)

C(5)	0.90463(14)	0.24779(9)	0.87682(9)	0.021(1)
C(6)	1.03791(15)	0.22791(11)	0.86299(10)	0.027(1)
C(7)	0.70738(12)	0.50213(9)	0.86504(8)	0.016(1)
C(8)	0.82542(13)	0.58030(9)	0.87297(9)	0.019(1)
C(9)	0.76939(14)	0.68215(10)	0.90648(10)	0.024(1)
C(10)	0.65807(16)	0.72995(11)	0.83882(11)	0.030(1)
C(11)	0.81733(12)	0.40345(9)	0.73696(8)	0.016(1)
C(12)	0.73413(13)	0.46065(10)	0.65848(9)	0.020(1)
C(13)	0.81166(16)	0.45296(11)	0.56784(9)	0.026(1)
C(14)	0.74688(17)	0.52043(11)	0.48932(10)	0.031(1)
P(1)	0.25852(3)	0.53499(2)	0.82557(2)	0.017(1)
F(1)	0.38800(8)	0.53640(7)	0.90504(5)	0.028(1)
F(2)	0.12929(8)	0.53368(7)	0.74665(6)	0.030(1)
F(3)	0.15485(8)	0.50086(7)	0.90402(6)	0.031(1)
F(4)	0.29096(10)	0.42005(7)	0.80370(7)	0.039(1)
F(5)	0.22639(11)	0.65057(7)	0.84820(7)	0.043(1)
F(6)	0.36346(10)	0.56954(9)	0.74800(6)	0.044(1)
H(1A)	0.5440	0.3696	0.7785	0.022
H(1B)	0.6398	0.2700	0.7846	0.022
H(2)	0.5341	0.3568	0.9522	0.026
H(3A)	0.5527	0.1570	0.8901	0.036
H(3B)	0.4927	0.1946	0.9905	0.036
H(4A)	0.9398	0.3962	0.9121	0.021
H(4B)	0.8130	0.3469	0.9651	0.021
H(5)	0.8369	0.1949	0.8696	0.025
H(6A)	1.1070	0.2799	0.8699	0.033
H(6B)	1.0649	0.1615	0.8461	0.033
H(7A)	0.6300	0.5283	0.8212	0.020
H(7B)	0.6691	0.4945	0.9279	0.020
H(8A)	0.8649	0.5890	0.8106	0.023
H(8B)	0.9024	0.5564	0.9183	0.023
H(9A)	0.7287	0.6722	0.9683	0.029
H(9B)	0.8500	0.7296	0.9163	0.029
H(10A)	0.6411	0.7997	0.8585	0.045
H(10B)	0.5699	0.6912	0.8393	0.045
H(10C)	0.6911	0.7299	0.7748	0.045
H(11A)	0.8330	0.3336	0.7148	0.020
H(11B)	0.9114	0.4357	0.7479	0.020
H(12A)	0.7247	0.5325	0.6766	0.024
H(12B)	0.6380	0.4315	0.6481	0.024
H(13A)	0.9120	0.4722	0.5817	0.032
H(13B)	0.8093	0.3819	0.5458	0.032
H(14A)	0.7952	0.5088	0.4314	0.046
H(14B)	0.7576	0.5914	0.5082	0.046
H(14C)	0.6461	0.5045	0.4778	0.046

Table T4. Anisotropic displacement parameters (Å^2) for uvic1601. The anisotropic displacement factor exponent takes the form: $-2\pi^2[h^2a^{*2}U_{11} + ... + 2hka^*b^*U_{12}]$.

	U_{11}	U_{22}	U_{33}	U_{23}	U_{13}	U_{12}
N(1)	0.0128(4)	0.0158(5)	0.0155(5)	-0.0008(4)	0.0016(4)	0.0002(4)
C(1)	0.0147(5)	0.0189(6)	0.0205(6)	-0.0011(4)	0.0016(4)	-0.0031(4)
C(2)	0.0186(6)	0.0225(6)	0.0243(6)	-0.0018(5)	0.0065(5)	-0.0021(5)
C(3)	0.0347(8)	0.0258(7)	0.0321(7)	0.0024(6)	0.0138(6)	-0.0017(6)
C(4)	0.0176(6)	0.0193(6)	0.0156(5)	0.0005(4)	-0.0009(4)	0.0020(4)
C(5)	0.0241(6)	0.0178(6)	0.0191(6)	0.0011(4)	-0.0018(5)	0.0021(5)
C(6)	0.0266(7)	0.0261(7)	0.0283(7)	-0.0029(5)	-0.0004(5)	0.0068(5)
C(7)	0.0155(5)	0.0156(5)	0.0186(6)	-0.0020(4)	0.0038(4)	0.0017(4)
C(8)	0.0178(6)	0.0173(6)	0.0232(6)	-0.0012(5)	0.0028(5)	-0.0004(4)
C(9)	0.0240(6)	0.0196(6)	0.0292(7)	-0.0040(5)	0.0013(5)	-0.0001(5)
C(10)	0.0358(8)	0.0228(7)	0.0319(7)	0.0011(6)	-0.0013(6)	0.0024(6)
C(11)	0.0155(5)	0.0198(6)	0.0146(5)	-0.0005(4)	0.0037(4)	0.0007(4)
C(12)	0.0203(6)	0.0228(6)	0.0167(5)	0.0006(5)	0.0014(4)	0.0006(5)
C(13)	0.0332(7)	0.0292(7)	0.0174(6)	0.0003(5)	0.0055(5)	0.0046(6)
C(14)	0.0411(8)	0.0333(8)	0.0185(6)	0.0020(5)	0.0028(6)	0.0007(6)
P(1)	0.0148(2)	0.0198(2)	0.0169(2)	0.0008(1)	0.0022(1)	-0.0013(1)
F(1)	0.0183(4)	0.0438(5)	0.0215(4)	0.0003(3)	-0.0015(3)	-0.0024(3)
F(2)	0.0219(4)	0.0416(5)	0.0242(4)	0.0022(3)	-0.0049(3)	-0.0018(3)
F(3)	0.0190(4)	0.0483(5)	0.0256(4)	0.0072(4)	0.0076(3)	-0.0026(4)
F(4)	0.0381(5)	0.0280(5)	0.0501(6)	-0.0133(4)	-0.0013(4)	0.0109(4)
F(5)	0.0610(6)	0.0199(4)	0.0459(5)	-0.0022(4)	-0.0095(5)	0.0060(4)
F(6)	0.0310(5)	0.0787(7)	0.0217(4)	0.0063(4)	0.0066(4)	-0.0227(5)

Table T5. Bond lengths [Å] for uvic1601.

atom-atom	distance	atom-atom	distance
N(1)-C(11)	1.5182(14)	N(1)-C(4)	1.5240(15)
N(1)-C(7)	1.5246(15)	N(1)-C(1)	1.5256(15)
C(1)-C(2)	1.4961(17)	C(1)-H(1A)	0.9900
C(1)-H(1B)	0.9900	C(2)-C(3)	1.3183(19)
C(2)-H(2)	0.9500	C(3)-H(3A)	0.9500
C(3)-H(3B)	0.9500	C(4)-C(5)	1.4996(17)
C(4)-H(4A)	0.9900	C(4)-H(4B)	0.9900
C(5)-C(6)	1.3168(19)	C(5)-H(5)	0.9500
C(6)-H(6A)	0.9500	C(6)-H(6B)	0.9500
C(7)-C(8)	1.5210(17)	C(7)-H(7A)	0.9900
C(7)-H(7B)	0.9900	C(8)-C(9)	1.5356(17)
C(8)-H(8A)	0.9900	C(8)-H(8B)	0.9900
C(9)-C(10)	1.5131(19)	C(9)-H(9A)	0.9900
C(9)-H(9B)	0.9900	C(10)-H(10A)	0.9800
C(10)-H(10B)	0.9800	C(10)-H(10C)	0.9800
C(11)-C(12)	1.5196(16)	C(11)-H(11A)	0.9900
C(11)-H(11B)	0.9900	C(12)-C(13)	1.5271(17)
C(12)-H(12A)	0.9900	C(12)-H(12B)	0.9900
C(13)-C(14)	1.5221(19)	C(13)-H(13A)	0.9900

C(13)-H(13B)	0.9900	C(14)-H(14A)	0.9800
C(14)-H(14B)	0.9800	C(14)-H(14C)	0.9800
P(1)-F(4)	1.5862(9)	P(1)-F(5)	1.5960(9)
P(1)-F(3)	1.5988(8)	P(1)-F(6)	1.5993(9)
P(1)-F(2)	1.5993(8)	P(1)-F(1)	1.6062(8)

Symmetry transformations used to generate equivalent atoms:

Table T6. Bond angles [°] for uvic1601.

atom-atom-atom	angle	atom-atom-atom	angle
C(11)-N(1)-C(4)	108.26(9)	C(11)-N(1)-C(7)	111.81(9)
C(4)-N(1)-C(7)	109.10(9)	C(11)-N(1)-C(1)	108.79(9)
C(4)-N(1)-C(1)	110.51(9)	C(7)-N(1)-C(1)	108.39(9)
C(2)-C(1)-N(1)	113.92(10)	C(2)-C(1)-H(1A)	108.8
N(1)-C(1)-H(1A)	108.8	C(2)-C(1)-H(1B)	108.8
N(1)-C(1)-H(1B)	108.8	H(1A)-C(1)-H(1B)	107.7
C(3)-C(2)-C(1)	122.02(12)	C(3)-C(2)-H(2)	119.0
C(1)-C(2)-H(2)	119.0	C(2)-C(3)-H(3A)	120.0
C(2)-C(3)-H(3B)	120.0	H(3A)-C(3)-H(3B)	120.0
C(5)-C(4)-N(1)	113.43(10)	C(5)-C(4)-H(4A)	108.9
N(1)-C(4)-H(4A)	108.9	C(5)-C(4)-H(4B)	108.9
N(1)-C(4)-H(4B)	108.9	H(4A)-C(4)-H(4B)	107.7
C(6)-C(5)-C(4)	122.17(12)	C(6)-C(5)-H(5)	118.9
C(4)-C(5)-H(5)	118.9	C(5)-C(6)-H(6A)	120.0
C(5)-C(6)-H(6B)	120.0	H(6A)-C(6)-H(6B)	120.0
C(8)-C(7)-N(1)	115.52(9)	C(8)-C(7)-H(7A)	108.4
N(1)-C(7)-H(7A)	108.4	C(8)-C(7)-H(7B)	108.4
N(1)-C(7)-H(7B)	108.4	H(7A)-C(7)-H(7B)	107.5
C(7)-C(8)-C(9)	110.59(10)	C(7)-C(8)-H(8A)	109.5
C(9)-C(8)-H(8A)	109.5	C(7)-C(8)-H(8B)	109.5
C(9)-C(8)-H(8B)	109.5	H(8A)-C(8)-H(8B)	108.1
C(10)-C(9)-C(8)	114.26(11)	C(10)-C(9)-H(9A)	108.7
C(8)-C(9)-H(9A)	108.7	C(10)-C(9)-H(9B)	108.7
C(8)-C(9)-H(9B)	108.7	H(9A)-C(9)-H(9B)	107.6
C(9)-C(10)-H(10A)	109.5	C(9)-C(10)-H(10B)	109.5
H(10A)-C(10)-H(10B)	109.5	C(9)-C(10)-H(10C)	109.5
H(10A)-C(10)-H(10C)	109.5	H(10B)-C(10)-H(10C)	109.5
N(1)-C(11)-C(12)	115.91(10)	N(1)-C(11)-H(11A)	108.3
C(12)-C(11)-H(11A)	108.3	N(1)-C(11)-H(11B)	108.3
C(12)-C(11)-H(11B)	108.3	H(11A)-C(11)-H(11B)	107.4
C(11)-C(12)-C(13)	109.15(10)	C(11)-C(12)-H(12A)	109.9
C(13)-C(12)-H(12A)	109.9	C(11)-C(12)-H(12B)	109.9
C(13)-C(12)-H(12B)	109.9	H(12A)-C(12)-H(12B)	108.3
C(14)-C(13)-C(12)	112.56(12)	C(14)-C(13)-H(13A)	109.1
C(12)-C(13)-H(13A)	109.1	C(14)-C(13)-H(13B)	109.1
C(12)-C(13)-H(13B)	109.1	H(13A)-C(13)-H(13B)	107.8
C(13)-C(14)-H(14A)	109.5	C(13)-C(14)-H(14B)	109.5
H(14A)-C(14)-H(14B)	109.5	C(13)-C(14)-H(14C)	109.5
H(14A)-C(14)-H(14C)	109.5	H(14B)-C(14)-H(14C)	109.5

F(4)-P(1)-F(5)	179.65(6)	F(4)-P(1)-F(3)	90.10(5)
F(5)-P(1)-F(3)	89.77(6)	F(4)-P(1)-F(6)	90.09(6)
F(5)-P(1)-F(6)	90.03(6)	F(3)-P(1)-F(6)	179.37(5)
F(4)-P(1)-F(2)	90.11(5)	F(5)-P(1)-F(2)	90.22(5)
F(3)-P(1)-F(2)	90.41(5)	F(6)-P(1)-F(2)	90.20(5)
F(4)-P(1)-F(1)	89.98(5)	F(5)-P(1)-F(1)	89.69(5)
F(3)-P(1)-F(1)	89.46(4)	F(6)-P(1)-F(1)	89.93(5)
F(2)-P(1)-F(1)	179.84(5)		

Symmetry transformations used to generate equivalent atoms:

Table T7. Torsion angles [°] for uvic1601.

atom-atom-atom-atom	angle	atom-atom-atom-atom	angle
C(11)-N(1)-C(1)-C(2)	168.74(10)	C(4)-N(1)-C(1)-C(2)	50.02(13)
C(7)-N(1)-C(1)-C(2)	-69.48(12)	N(1)-C(1)-C(2)-C(3)	-125.65(14)
C(11)-N(1)-C(4)-C(5)	-58.34(13)	C(7)-N(1)-C(4)-C(5)	179.78(10)
C(1)-N(1)-C(4)-C(5)	60.71(13)	N(1)-C(4)-C(5)-C(6)	118.02(13)
C(11)-N(1)-C(7)-C(8)	-54.96(13)	C(4)-N(1)-C(7)-C(8)	64.74(12)
C(1)-N(1)-C(7)-C(8)	-174.87(10)	N(1)-C(7)-C(8)-C(9)	179.10(10)
C(7)-C(8)-C(9)-C(10)	-63.35(15)	C(4)-N(1)-C(11)-C(12)	-172.25(10)
C(7)-N(1)-C(11)-C(12)	-52.05(13)	C(1)-N(1)-C(11)-C(12)	67.63(13)
N(1)-C(11)-C(12)-C(13)	-176.22(10)	C(11)-C(12)-C(13)-C(14)	-171.86(12)

Symmetry transformations used to generate equivalent atoms:

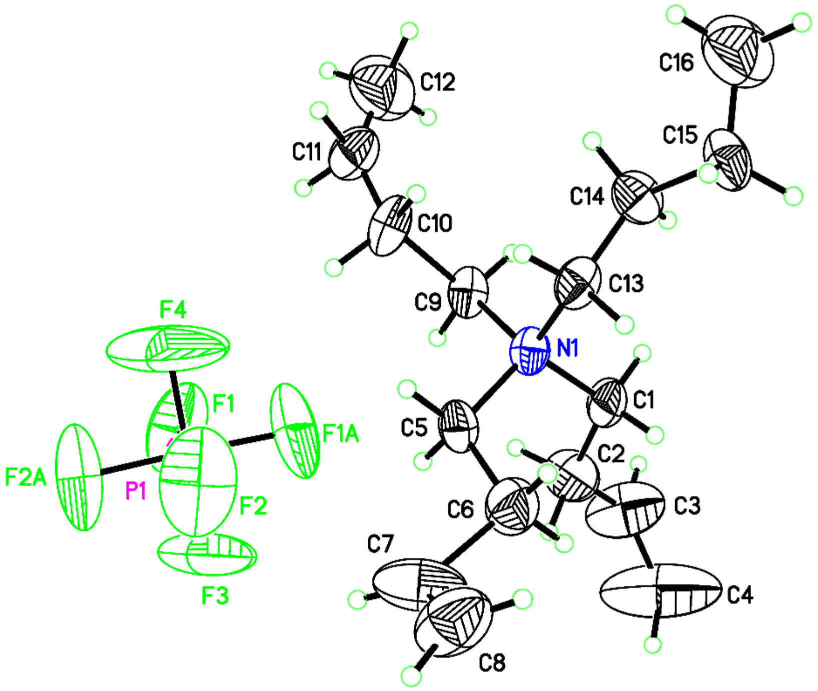

Figure S38. X-ray crystal structure of **R7.**

DISCUSSION

The compound crystallizes as colourless tablet-like crystals. There are four molecules of the di-n-butyl, di-butylene ammonium hexafluorophosphate salt in the unit cell of the primitive, centrosymmetric, orthorhombic space group Pnma.

Both the cation and the anion crystallize on the crystallographic mirror planes, perpendicular to the b axis. Because of this location, only half of each molecule is observed within the asymmetric unit. Furthermore, the cation is disordered about the mirror plane. It was ultimately modeled with a half occupancy molecule with the two parts of the disorder decoupled from each other. Due to this decoupling, C12 and C16 are directly related and refined poorly. Thus they were restrained to have the same atomic displacement parameters and constrained to have similar C-C distances to their respective bonding methylene carbon atom. This disorder also disguises the true location of the ethylene functionality. The model depicted here was developed comparing bond distances and angles of residual density to the gamma carbon of the butyl chains. It is likely that all four sites have some character of methyl and terminal ethylinic character. Furthermore, the PF_6 anion also exhibits typical elongation, bordering on positional disorder, of the fluorine atoms.

Attempts to solve the structure in lower symmetry space groups (primarily $Pna2_1$, the acentric isomorph of Pnma) did not yield satisfactory results and were abandoned.

Bond distances and angles are generally reliable. However, as noted above there is the real possibility that the terminal groups (methyl and ethylene) are scrambled.

CRYSTAL SUMMARY

Crystal data for $C_{16}H_{32}F_6NP$; M_r = 383.39; Orthorhombic; space group Pnma; a = 15.2010(18) Å; b = 9.7668(12) Å; c = 13.4419(16) Å; α = 90°; β = 90°; γ = 90°; V = 1995.7(4) $Å^3$; Z = 4; T = 120(2) K; λ(Mo-Kα) = 0.71073 Å; μ(Mo-Kα) = 0.189 mm^{-1}; d_{calc} = 1.276g.cm^{-3}; 33098 reflections collected; 2168 unique (R_{int} = 0.0510); giving R_1 = 0.0867, wR_2 = 0.2361 for 1582 data with [I>2σ(I)] and R_1 = 0.1111, wR_2 = 0.2583 for all 2168 data. Residual electron density (e^-.$Å^{-3}$) max/min: 0.723/-0.515.

An arbitrary sphere of data were collected on a colorless tablet-like crystal, having approximate dimensions of 0.138 × 0.132 × 0.078 mm, on a Bruker APEX-II diffractometer using a combination of ω- and φ-scans of 0.5°.[2] Data were corrected for absorption and polarization effects and analyzed for space group determination. The structure was solved by intrinsic phasing methods and expanded routinely.[3] The model was refined by full-matrix least-squares analysis of F^2 against all reflections.[4] All non-hydrogen atoms were refined with anisotropic atomic displacement parameters. Unless otherwise noted, hydrogen atoms were included in calculated positions. Atomic displacement parameters for the hydrogens were tied to the equivalent isotropic displacement parameter of the atom to which they are bonded (U_{iso}(H) = 1.5U_{eq}(C) for methyl, 1.2U_{eq}(C) for all others).

Table T8. Crystal data and structure refinement for uvic1602.

Identification code	uvic1602	
Empirical formula	$C_{16}H_{32}F_6NP$	
Formula weight	383.39	
Temperature	120(2) K	
Wavelength	0.71073 Å	
Crystal system	Orthorhombic	
Space group	Pnma	
Unit cell dimensions	a = 15.2010(18) Å	α = 90°
	b = 9.7668(12) Å	β = 90°
	c = 13.4419(16) Å	γ = 90°
Volume	1995.7(4) $Å^3$	
Z	4	
Density (calculated)	1.276 g.cm^{-3}	
Absorption coefficient (μ)	0.189 mm^{-1}	
F(000)	816	
Crystal color, habit	colorless, tablet	
Crystal size	0.138 × 0.132 × 0.078 mm^3	
θ range for data collection	2.022 to 26.374°	
Index ranges	-19 ≤ h ≤ 19, -12 ≤ k ≤ 12, -16 ≤ l ≤ 16	
Reflections collected	33098	
Independent reflections	2168 [R_{int} = 0.0510]	
Completeness to θ = 25.242°	100.0 %	
Absorption correction	Numerical	
Max. and min. transmission	1.0000 and 0.9488	
Refinement method	Full-matrix least-squares on F^2	
Data / restraints / parameters	2168 / 1 / 183	
Goodness-of-fit on F^2	1.055	
Final R indices [I>2σ(I)]	R_1 = 0.0867, wR_2 = 0.2361	

R indices (all data)	R_1 = 0.1111, wR_2 = 0.2583
Extinction coefficient	n/a
Largest diff. peak and hole	0.723 and -0.515 $e^{-}.Å^{-3}$

Table T9. Atomic coordinates and equivalent isotropic displacement parameters ($Å^2$) for uvic1602. U(eq) is defined as one third of the trace of the orthogonalized U_{ij} tensor.

	x	y	z	U(eq)
N(1)	0.1904(2)	0.7500	0.4714(3)	0.034(1)
C(1)	0.2816(4)	0.8002(7)	0.4461(5)	0.043(2)
C(2)	0.3578(4)	0.7074(9)	0.4727(6)	0.064(3)
C(3)	0.4427(5)	0.724(3)	0.4373(7)	0.082(9)
C(4)	0.5203(6)	0.758(5)	0.4767(7)	0.151(8)
C(5)	0.1845(4)	0.7036(6)	0.5805(5)	0.040(2)
C(6)	0.2111(6)	0.8142(9)	0.6548(6)	0.057(2)
C(7)	0.2046(5)	0.741(4)	0.7614(6)	0.081(5)
C(8)	0.1883(7)	0.8379(13)	0.8159(8)	0.086(3)
C(9)	0.1734(4)	0.6210(6)	0.4059(5)	0.037(1)
C(10)	0.0804(5)	0.5626(7)	0.4142(6)	0.048(2)
C(11)	0.0495(9)	0.4757(18)	0.3399(12)	0.054(3)
C(12)	0.0505(13)	0.4550(17)	0.2350(14)	0.098(5)
C(13)	0.1237(5)	0.8588(6)	0.4515(5)	0.040(2)
C(14)	0.1128(5)	0.9006(7)	0.3448(5)	0.047(2)
C(15)	0.0764(9)	1.0563(17)	0.3411(14)	0.053(4)
C(16)	0.0216(13)	1.0611(18)	0.2555(14)	0.098(5)
P(1)	0.19523(8)	0.2500	0.61424(9)	0.038(1)
F(1)	0.2338(2)	0.1395(3)	0.5425(3)	0.110(1)
F(2)	0.1586(3)	0.3587(4)	0.6889(3)	0.131(2)
F(3)	0.2835(3)	0.2500	0.6704(3)	0.137(3)
F(4)	0.1079(3)	0.2500	0.5581(4)	0.200(4)
H(1A)	0.2907	0.8890	0.4801	0.052
H(1B)	0.2839	0.8178	0.3736	0.052
H(2A)	0.3621	0.7082	0.5461	0.076
H(2B)	0.3397	0.6136	0.4537	0.076
H(3)	0.4466	0.7080	0.3677	0.098
H(4A)	0.5247	0.7767	0.5459	0.181
H(4B)	0.5710	0.7631	0.4357	0.181
H(5A)	0.1233	0.6749	0.5948	0.048
H(5B)	0.2229	0.6228	0.5900	0.048
H(6A)	0.1707	0.8934	0.6511	0.069
H(6B)	0.2719	0.8461	0.6418	0.069
H(7)	0.2116	0.6467	0.7779	0.097
H(8A)	0.1831	0.9273	0.7887	0.103
H(8B)	0.1807	0.8240	0.8853	0.103
H(9A)	0.1848	0.6449	0.3355	0.044
H(9B)	0.2159	0.5489	0.4251	0.044
H(10A)	0.0767	0.5125	0.4781	0.058
H(10B)	0.0392	0.6409	0.4187	0.058
H(11A)	-0.0144	0.4755	0.3538	0.065
H(11B)	0.0704	0.3857	0.3641	0.065

H(12A)	0.0357	0.3595	0.2203	0.147
H(12B)	0.1092	0.4758	0.2090	0.147
H(12C)	0.0072	0.5155	0.2037	0.147
H(13A)	0.1399	0.9409	0.4905	0.048
H(13B)	0.0661	0.8264	0.4764	0.048
H(14A)	0.0708	0.8385	0.3111	0.056
H(14B)	0.1700	0.8948	0.3098	0.056
H(15A)	0.0423	1.0779	0.4019	0.064
H(15B)	0.1255	1.1222	0.3351	0.064
H(16A)	0.0049	1.1562	0.2420	0.147
H(16B)	-0.0315	1.0064	0.2673	0.147
H(16C)	0.0535	1.0239	0.1983	0.147

Table T10. Anisotropic displacement parameters (Å^2) for uvic1602.
The anisotropic displacement factor exponent takes the form:
$-2\pi^2[h^2a^{*2}U_{11} + ... + 2hka^*b^*U_{12}]$

	U_{11}	U_{22}	U_{33}	U_{23}	U_{13}	U_{12}
N(1)	0.0318(19)	0.0309(18)	0.040(2)	0.000	0.0081(15)	0.000
C(1)	0.034(3)	0.045(4)	0.050(3)	0.009(3)	0.006(3)	-0.011(2)
C(2)	0.033(3)	0.094(9)	0.064(4)	0.023(4)	0.006(3)	-0.003(3)
C(3)	0.036(3)	0.13(3)	0.080(5)	-0.033(11)	0.009(3)	0.015(7)
C(4)	0.051(5)	0.32(2)	0.076(6)	-0.06(2)	-0.001(4)	0.051(19)
C(5)	0.046(3)	0.039(3)	0.037(3)	0.007(2)	0.010(3)	-0.004(2)
C(6)	0.064(5)	0.060(4)	0.048(4)	0.001(4)	0.003(4)	-0.012(4)
C(7)	0.070(5)	0.125(12)	0.046(4)	-0.029(12)	-0.010(4)	0.035(14)
C(8)	0.084(7)	0.104(8)	0.069(6)	-0.026(6)	0.005(6)	-0.023(6)
C(9)	0.036(3)	0.028(3)	0.047(3)	-0.003(3)	0.013(3)	0.004(2)
C(10)	0.045(4)	0.036(3)	0.063(4)	-0.013(3)	0.017(3)	-0.011(3)
C(11)	0.043(8)	0.061(9)	0.058(6)	-0.005(5)	0.007(6)	-0.010(6)
C(12)	0.088(12)	0.089(5)	0.117(8)	0.024(7)	-0.007(8)	0.018(5)
C(13)	0.039(3)	0.027(3)	0.054(4)	-0.010(3)	0.003(3)	0.002(3)
C(14)	0.052(4)	0.040(4)	0.049(4)	0.000(3)	0.002(3)	0.011(3)
C(15)	0.040(8)	0.048(7)	0.071(6)	0.023(5)	0.013(6)	0.009(5)
C(16)	0.088(12)	0.089(5)	0.117(8)	0.024(7)	-0.007(8)	0.018(5)
P(1)	0.0388(7)	0.0356(7)	0.0386(7)	0.000	-0.0056(5)	0.000
F(1)	0.131(3)	0.0613(18)	0.138(3)	-0.0506(18)	0.055(2)	-0.0237(18)
F(2)	0.160(3)	0.084(2)	0.148(3)	-0.038(2)	0.080(3)	0.013(2)
F(3)	0.071(3)	0.281(8)	0.061(3)	0.000	-0.028(2)	0.000
F(4)	0.052(3)	0.454(14)	0.093(4)	0.000	-0.029(3)	0.000

Table T11. Bond lengths [Å] for uvic1602.

atom-atom	distance	atom-atom	distance
N(1)-C(13)	1.493(7)	N(1)-C(1)	1.510(7)
N(1)-C(5)	1.538(7)	N(1)-C(9)	1.558(6)
C(1)-C(2)	1.514(10)	C(1)-H(1A)	0.9900
C(1)-H(1B)	0.9900	C(2)-C(3)	1.385(10)
C(2)-H(2A)	0.9900	C(2)-H(2B)	0.9900
C(3)-C(4)	1.334(19)	C(3)-H(3)	0.9500

C(4)-H(4A)	0.9500	C(4)-H(4B)	0.9500
C(5)-C(6)	1.525(10)	C(5)-H(5A)	0.9900
C(5)-H(5B)	0.9900	C(6)-C(7)	1.61(2)
C(6)-H(6A)	0.9900	C(6)-H(6B)	0.9900
C(7)-C(8)	1.22(3)	C(7)-H(7)	0.9500
C(8)-H(8A)	0.9500	C(8)-H(8B)	0.9500
C(9)-C(10)	1.528(9)	C(9)-H(9A)	0.9900
C(9)-H(9B)	0.9900	C(10)-C(11)	1.392(18)
C(10)-H(10A)	0.9900	C(10)-H(10B)	0.9900
C(11)-C(12)	1.424(15)	C(11)-H(11A)	0.9900
C(11)-H(11B)	0.9900	C(12)-H(12A)	0.9800
C(12)-H(12B)	0.9800	C(12)-H(12C)	0.9800
C(13)-C(14)	1.501(10)	C(13)-H(13A)	0.9900
C(13)-H(13B)	0.9900	C(14)-C(15)	1.619(19)
C(14)-H(14A)	0.9900	C(14)-H(14B)	0.9900
C(15)-C(16)	1.421(14)	C(15)-H(15A)	0.9900
C(15)-H(15B)	0.9900	C(16)-H(16A)	0.9800
C(16)-H(16B)	0.9800	C(16)-H(16C)	0.9800
P(1)-F(4)	1.528(4)	P(1)-F(3)	1.539(4)
P(1)-F(1)	1.562(3)	P(1)-F(1)#1	1.562(3)
P(1)-F(2)#1	1.563(3)	P(1)-F(2)	1.563(3)

Symmetry transformations used to generate equivalent atoms:
#1 x,-y+1/2,z

Table T12. Bond angles [°] for uvic1602.

atom-atom-atom	angle	atom-atom-atom	angle
C(13)-N(1)-C(1)	110.6(4)	C(13)-N(1)-C(5)	109.9(4)
C(1)-N(1)-C(5)	111.3(4)	C(13)-N(1)-C(9)	111.2(4)
C(1)-N(1)-C(9)	106.8(4)	C(5)-N(1)-C(9)	106.9(3)
N(1)-C(1)-C(2)	117.1(5)	N(1)-C(1)-H(1A)	108.0
C(2)-C(1)-H(1A)	108.0	N(1)-C(1)-H(1B)	108.0
C(2)-C(1)-H(1B)	108.0	H(1A)-C(1)-H(1B)	107.3
C(3)-C(2)-C(1)	124.1(13)	C(3)-C(2)-H(2A)	106.3
C(1)-C(2)-H(2A)	106.3	C(3)-C(2)-H(2B)	106.3
C(1)-C(2)-H(2B)	106.3	H(2A)-C(2)-H(2B)	106.4
C(4)-C(3)-C(2)	135.7(10)	C(4)-C(3)-H(3)	112.1
C(2)-C(3)-H(3)	112.1	C(3)-C(4)-H(4A)	120.0
C(3)-C(4)-H(4B)	120.0	H(4A)-C(4)-H(4B)	120.0
C(6)-C(5)-N(1)	113.6(5)	C(6)-C(5)-H(5A)	108.9
N(1)-C(5)-H(5A)	108.9	C(6)-C(5)-H(5B)	108.9
N(1)-C(5)-H(5B)	108.9	H(5A)-C(5)-H(5B)	107.7
C(5)-C(6)-C(7)	104.5(13)	C(5)-C(6)-H(6A)	110.8
C(7)-C(6)-H(6A)	110.8	C(5)-C(6)-H(6B)	110.8
C(7)-C(6)-H(6B)	110.8	H(6A)-C(6)-H(6B)	108.9
C(8)-C(7)-C(6)	101(2)	C(8)-C(7)-H(7)	129.3
C(6)-C(7)-H(7)	129.3	C(7)-C(8)-H(8A)	120.0
C(7)-C(8)-H(8B)	120.0	H(8A)-C(8)-H(8B)	120.0
C(10)-C(9)-N(1)	114.5(5)	C(10)-C(9)-H(9A)	108.6
N(1)-C(9)-H(9A)	108.6	C(10)-C(9)-H(9B)	108.6

N(1)-C(9)-H(9B)	108.6	H(9A)-C(9)-H(9B)	107.6
C(11)-C(10)-C(9)	119.2(8)	C(11)-C(10)-H(10A)	107.5
C(9)-C(10)-H(10A)	107.5	C(11)-C(10)-H(10B)	107.5
C(9)-C(10)-H(10B)	107.5	H(10A)-C(10)-H(10B)	107.0
C(10)-C(11)-C(12)	142.5(17)	C(10)-C(11)-H(11A)	101.3
C(12)-C(11)-H(11A)	101.3	C(10)-C(11)-H(11B)	101.3
C(12)-C(11)-H(11B)	101.3	H(11A)-C(11)-H(11B)	104.6
C(11)-C(12)-H(12A)	109.5	C(11)-C(12)-H(12B)	109.5
H(12A)-C(12)-H(12B)	109.5	C(11)-C(12)-H(12C)	109.5
H(12A)-C(12)-H(12C)	109.5	H(12B)-C(12)-H(12C)	109.5
N(1)-C(13)-C(14)	116.1(5)	N(1)-C(13)-H(13A)	108.3
C(14)-C(13)-H(13A)	108.3	N(1)-C(13)-H(13B)	108.3
C(14)-C(13)-H(13B)	108.3	H(13A)-C(13)-H(13B)	107.4
C(13)-C(14)-C(15)	108.8(8)	C(13)-C(14)-H(14A)	109.9
C(15)-C(14)-H(14A)	109.9	C(13)-C(14)-H(14B)	109.9
C(15)-C(14)-H(14B)	109.9	H(14A)-C(14)-H(14B)	108.3
C(16)-C(15)-C(14)	104.8(13)	C(16)-C(15)-H(15A)	110.8
C(14)-C(15)-H(15A)	110.8	C(16)-C(15)-H(15B)	110.8
C(14)-C(15)-H(15B)	110.8	H(15A)-C(15)-H(15B)	108.9
C(15)-C(16)-H(16A)	109.5	C(15)-C(16)-H(16B)	109.5
H(16A)-C(16)-H(16B)	109.5	C(15)-C(16)-H(16C)	109.5
H(16A)-C(16)-H(16C)	109.5	H(16B)-C(16)-H(16C)	109.5
F(4)-P(1)-F(3)	179.8(3)	F(4)-P(1)-F(1)	91.2(2)
F(3)-P(1)-F(1)	88.6(2)	F(4)-P(1)-F(1)#1	91.2(2)
F(3)-P(1)-F(1)#1	88.6(2)	F(1)-P(1)-F(1)#1	87.4(2)
F(4)-P(1)-F(2)#1	90.5(2)	F(3)-P(1)-F(2)#1	89.7(2)
F(1)-P(1)-F(2)#1	93.48(18)	F(1)#1-P(1)-F(2)#1	178.1(3)
F(4)-P(1)-F(2)	90.4(2)	F(3)-P(1)-F(2)	89.7(2)
F(1)-P(1)-F(2)	178.1(3)	F(1)#1-P(1)-F(2)	93.48(18)
F(2)#1-P(1)-F(2)	85.6(3)		

Symmetry transformations used to generate equivalent atoms:
#1 x,-y+1/2,z

Table T13. Torsion angles [°] for uvic1602.

atom-atom-atom-atom	angle	atom-atom-atom-atom	angle
C(13)-N(1)-C(1)-C(2)	173.5(6)	C(5)-N(1)-C(1)-C(2)	51.0(7)
C(9)-N(1)-C(1)-C(2)	-65.3(7)	N(1)-C(1)-C(2)-C(3)	166.3(12)
C(1)-C(2)-C(3)-C(4)	113(4)	C(13)-N(1)-C(5)-C(6)	-66.6(7)
C(1)-N(1)-C(5)-C(6)	56.4(7)	C(9)-N(1)-C(5)-C(6)	172.6(5)
N(1)-C(5)-C(6)-C(7)	-177.2(6)	C(5)-C(6)-C(7)-C(8)	-151.8(10)
C(13)-N(1)-C(9)-C(10)	-53.9(7)	C(1)-N(1)-C(9)-C(10)	-174.7(5)
C(5)-N(1)-C(9)-C(10)	66.0(6)	N(1)-C(9)-C(10)-C(11)	161.1(9)
C(9)-C(10)-C(11)-C(12)	-39(2)	C(1)-N(1)-C(13)-C(14)	64.8(7)
C(5)-N(1)-C(13)-C(14)	-171.8(5)	C(9)-N(1)-C(13)-C(14)	-53.6(7)
N(1)-C(13)-C(14)-C(15)	-154.1(6)	C(13)-C(14)-C(15)-C(16)	-146.7(12)

Symmetry transformations used to generate equivalent atoms:
#1 x,-y+1/2,z

References:

1. G. T. Thomas, S. Donnecke, I. C. Chagunda, J. S. McIndoe, Chemistry Methods 2022, 2, e202100068.

2. Bruker AXS. (2014). *APEX-2*. Bruker-Nonius AXS, Madison, Wisconsin, USA.

3. G. M. Sheldrick, *Acta Cryst.*, **2015**, *A71*, 3.

4. G. M. Sheldrick, *Acta Cryst.*, **2015**, *C71*, 3.